UNIVERSITY OF CALIFORNIA
RIVERSIDE

Development of a Flow-Cytometric Screening Method for MMP-14 Inhibitory Antibody

A Thesis submitted in partial satisfaction
of the requirements for the degree of

Master of Science

in

Chemical and Environmental Engineering

by

Kuili Fang

August 2014

Thesis Committee:
Dr. Xin Ge, Chairperson
Dr. Ashok Mulchandani
Dr. Huiwang Ai

The Thesis of Kuili Fang is approved:

_____

_____

_____

Committee Chairperson

University of California, Riverside

Acknowledgement

I would like to thank my advisor, Prof. Xin Ge for his continuous support and encouragement through all my Master's Degree. Thank you for trusting me when I started this project. I am so fortunate to have your guide when I had difficulty with my experiment. You gave me many chances to be creative, hard-working and responsible. I would like to express my sincere gratitude to you. Thank you.

My heartfelt appreciation goes to lab member, Peter Nam, for his valuable comments and suggestions on this project when I was a new man to the molecular biology field. Thanks to Diana Perez for helping me clone the DNA antibody libraries. Thank you.

Special thanks go to my parents who have always provided the love and necessary support for me to progress to this stage in my life. Thank you for your generosity and help by supporting and encouraging me to work hard and succeed. No words can express how grateful I am for all of your love. Thank you.

ABSTRACT OF THE THESIS

Development of a Flow-Cytometric Screening Method for MMP-14 Inhibitory Antibody

by

Kuili Fang

Master of Science, Graduate Program in Chemical and Environmental Engineering
University of California, Riverside, August 2014
Dr. Xin Ge, Chairperson

Mounting evidence suggests that MMP-14 (Matrix Metalloproteinase-14) plays an important role in cancer proliferation, invasion and migration to other healthy tissues through its extracellular matrix degradation activity. Toward the discovery of MMP-14 inhibitors, antibodies are emerging as a very attractive approach, due to their high specificity, low side effects and excellent in vivo stability. However, most current antibody selection methods are essentially binding assays with little control on inhibition function. Here, we report the development of a functional high-throughput screening method, which is able to identify inhibitory clones from non-specific or non-inhibitory clones. This novel method is based on antibody yeast display and dual color fluorescence-activated cell sorting (FACS). More specifically, the catalytic domain of MMP-14 and its native inhibitor N-TIMP-2 (N-terminal-domain of Tissue inhibitor of metalloproteinases-2) were successfully cloned, expressed, purified and refolded to their active formats, then conjugated with fluorophores Alexa488 and Alexa647 respectively. Yeast cells displaying various antibody clones were subjected to incubate with Alexa488-

MMP-14 and Alexa647-N-TIMP-2. Dual Color FACS scanning results clearly demonstrated that the inhibitory antibody cells (DX-2400, 1F8) exhibited high Alexa488 fluorescence signals and low Alexa647 fluorescence signals, while the specific but non-inhibitory antibody cells (3B1, 2A10) exhibited high signals on both Alexa488 and Alexa647, and non-specific antibody cells (1H11, 2D9, 2F9, 1B11, b12, M18) exhibited low signals on both fluorophores. This proof-of-concept study paves the way for utilizing this functional screening method to isolate inhibitory antibodies from affinity maturation and synthetic antibody libraries in future researches.

Table of Contents

List of Figures

List of Tables

1 Introduction

1.1 MMP-14 is a promising anti-cancer target

The intracellular pathways and main activities of cancer cells including autonomous growth, replication, invasions of tissues around and metastasis, are always the key factors of study for the developments of therapeutic methods (Hidalgo et al., 2001). Matrix metalloproteinases (MMPs) are a family of zinc-ion dependent endopeptidases (26 members), which can mainly regulate these cancer cell behaviors and achieve an environment that supports the cancer cell activities such as growth, invasions and migrations by degrading the physical barriers like extracellular matrix (ECM) (Chambers and Matrisian, 1997). All the MMPs except the MMP-7 and MMP-26 (absence of hinge region and haemopexin domain), have the similar structure which contains a signal peptide, a propeptide domain, a catalytic domain with a zinc active site, a hinge region and a haemopexin domain. Besides, fibronectin type II inserts are in the catalytic domain of MMP-2 and MMP-9, and all the membrane type matrix metalloproteinases (MT-MMPs) have additionally a transmembrane domain (**Figure 1.1**) (Murphy and Knäuper, 1997). Functional mature MMPs are activated from their pro-MMPs, which are secreted as latent precursors then activated in the cellular space. The pro-MMPs are inactivated by the interactions between the propeptide and the catalytic domain, preventing the substrate entering the catalytic reaction pocket. Once the propeptide is proteolytic-location partially cleaved, the reaction pocket is exposed to the substrate and MMP is activated (Murphy et al., 1999).

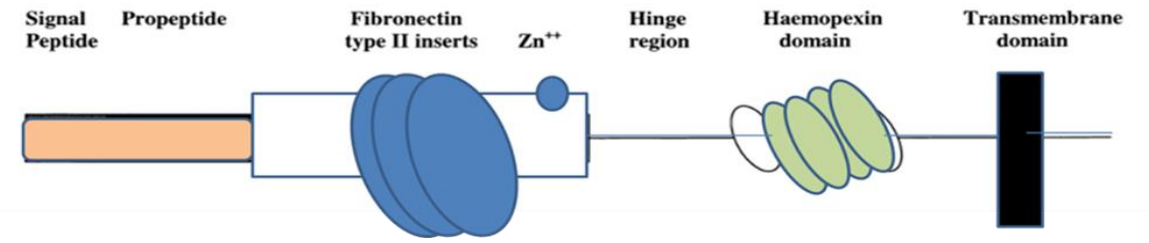

Figure 1.1 General structure of matrix metalloproteinases (MMPs) (Hidalgo et al., 2001).

As subfamily members of MMPs, MT-MMPs contain extra transmembrane domains or glycosylphosphatidylinositol comparing to general MMP structure (Sternlicht and Werb, 2001). Because of the extra domains, MT-MMPs are tethered at cancer cell membranes and help the cancer cells to reach and degrade the ECM, and activate other MMPs that bind to ECM. In this way, the special locations and functions make the MT-MMPs more important in the remodeling the ECM, cancer cell invasion and metastasis (Nakahara et al., 1997). MMP-14, another name MT1-MMP, is one of the MT-MMPs, whose degradation of ECM leads to the proliferation, invasion and migration of cancer cells (Tomari et al., 2009). Additionally, MMP-14 can activate the pro-MMP-2 via tissue inhibitor of metalloproteinase 2 (TIMP-2) to enhance the degradation of ECM. TIMP-2 contains two domains: N-terminal domain and C-terminal domain. During the process of activating pro-MMP-2, TIMP-2's N-terminal domain binds to and inhibits the catalytic domain of MMP-14, and its C-terminal domain has the non-covalent interaction with the haemopexin domain of pro-MMP-2 (Murphy et al., 1992; Willenbrock et al., 1993). After the MMP-14-TIMP-2-pro-MMP-2 complex is formed, another MMP-14 forms a dimer with the first MMP-14, and cleaves the pro-MMP-2 to obtain the mature MMP-2 (Sato et al., 1994).

1.2 Development of highly specific and highly potent MMP-14 inhibitors is challenging

MMP-14 is a promising drug target for cancer treatment, not only due to its extracellular location on membrane of cancer cells, but also its regulatory functions on cancer cell physiological activities (Tomari et al., 2009). However, previous attempts focusing on development of chemical compound inhibitors, *e.g.*, hydroxamates, targeting broad-spectrum MMPs all failed in clinical trials due to severe side effects (Turk, 2006). It is now known that MMPs play more complex and paradoxical roles in tumor progression beyond simple ECM degradation (Overall and Kleifeld, 2006; Kessenbrock et al., 2010). While many facets of proteolytic action are pro-tumorigenic, some MMPs indeed exhibit anti-tumorigenic effects in certain circumstances (Egeblad and Werb, 2002; Decock et al., 2011). For these reasons, selectively blocking tumorigenesis-promoting MMPs but not tumorigenesis-suppressing MMPs is highly desired for a successful therapy. However, the catalytic domains of 26 MMP family members share high amino acid similarity, and their active sites are extensively conserved. Therefore, it is extraordinarily difficult to distinguish tumorigenic and tumor-suppressing MMPs with small molecule inhibitors (Zucker and Cao, 2009; Turk, 2006).

Toward more specific MMP-14 inhibition, efforts have been made for the developments biologic-based inhibitors, which include proteins, peptides and antibodies. The early inhibitors of MMP-14 are mainly the TIMP family, α2-macroglobulin (α2M) and reversion-inducing cysteine-rich protein with Kazal motifs (RECK) (Zucker et al., 2003). The TIMP family (except TIMP-1's weak inhibition function) inhibits MMP-14

enzyme activities by binding to the catalytic zinc through reversible interactions but TIMPs can bind to other MMPs besides MMP-14 (Murphy et al., 1992; Fernandez-Catalan et al., 1998). α2M has irreversible inhibition functions with nearly all the MMPs, so neither TIMPs nor α2M is specific to MMP-14 (Zucker et al., 1999). RECK can suppress the cancer cell growth, invasion and migration by only inhibiting MMP-2, MMP-9 and MMP-14, and has good effects in the tumor clinical research (Takemotoa et al., 2007). Recently, different peptides have been studied to inhibit the MMP-14 functions. IS4 (VMDGYPMP), IVS4 (GYPKSALR), which are from the outermost strand of MMP-14 haemopexin domain blade, and peptide G (GACFSIAHECGA), which is from phage display libraries, effectively suppress the MMP-14 activities related to cancer cell metastasis. Peptide G is also a selective inhibitor for MMP-14 with IC_{50}~100 μM, but IS4 and IVS4 can inhibit other MMPs (Ndinguri et al., 2012).

Antibody-based inhibitors are emerging as very attractive therapeutic agents because of: (1) high affinity and high specificity due to the large antigen-antibody interactions area provided by multiple complementarity-determining regions (CDRs); (2) extended half-life and the well-known mechanisms of antibody action; (3) low immunogenicity and low toxicity; (4) a large number of proteases potentially targetable by antibodies, since ~50% of human proteases are extracellular. Monoclonal antibodies DX-2400 and 9E8 have been generated and showed their specificities to MMP-14. DX-2400 was developed from human Fab displaying phage library with IC_{50}~2nM, and showed effective repression on tumor cell activities on the test of mouse lung (Devy et al., 2009). The mAb 9E8 is an interesting antibody because it can stop the MMP-14

activating MMP-2 but couldn't inhibit the MMP-14 enzyme activity. The study showed that mAb 9E8 could bind to catalytic domain but not the substrate binding region, so it could obstruct the TIMP-2 (has the interaction with pro-MMP-2) binding to MMP-14 but had no effect on the MMP-14 degradation functions (Shiryaev et al., 2013).

Current technology of antibody selection is essential for binding-based assays. The challenge is that these selection methods have little control on epitope specificity or inhibitory functions. This study aims to develop a function-based high-throughput screening method to efficiently identify inhibitory antibodies. Unlike binding-based assays, function-based HTS will significantly increase the possibility to enrich inhibitory mAbs.

1.3 Antibody and its selection methods

Antibodies, other name immunoglobulins, are protein monomers like Y shape, or dimmer or pentamers of this kind of molecules (Wang et al., 2006). Native antibodies' structures contain two regions, the variable region (V region) and the constant region (C region). The V region is at the top of such Y-shape antibodies and has the affinity to the antigens. The C region is at the bottom of antibodies and mediates immune activities through connection with effector cells (Janeway et al., 2001). There are 5 classes of antibodies, IgA, IgD, IgE, IgM and IgG according to different C regions, named, α, δ, ε, μ, and γ respectively and their different sizes (IgG, IgA and IgM are monomer, dimmer and pentamer respectively) (Wang et al., 2006). The IgG (**Figure 1.2**), the most common

type of antibody, has two heavy chains (H chains) and two light chains (L chains), linked together by multiple disulfide bonds (Harris et al., 2004; Janeway et al., 2001).

More and more antibodies have been developed as drugs for cancer and immunological diseases (Reichert, 2008), due to their high specificity, high affinity, low side effects and excellent stability in vivo (Wu and Kabat, 1970). The successful rate of the antibody approval by FDA (Food and Drug Administration) is considerably higher than that of small compounds. For example, humanized mAbs that entered clinical study during 1988 to 2006 had an overall success FDA approval rate of 17% (Reichert, 2008).

For researches of antibody library construction and selection, functional fragments of antibodies are often used instead of the full size antibodies. One of such particular regions called fragment antigen binding (Fab) is in charge of antigen binding (**Figure 1.2**). Fab contains one light chain and part of heavy chain (constant domain 1 and variable domain from the heavy chain) (Cacia et al., 1996). Another commonly used fragment, the single-chain variable fragment (scFv) is formed by linking the variable domains of heavy chain (V_H) and light chain (V_L) with a flexible linker (**Figure 1.2**) (Bird et al., 1988). Fab and scFv are smaller than full size immunoglobulins but contain the antigen affinity and specificity characters, thus widely used in methodology developments for antibody selections including phage display and yeast surface display (Hoogenboom et al., 1991; Cacia et al., 1996; Boder and Wittrup, 1997; Kondo and Ueda, 2004).

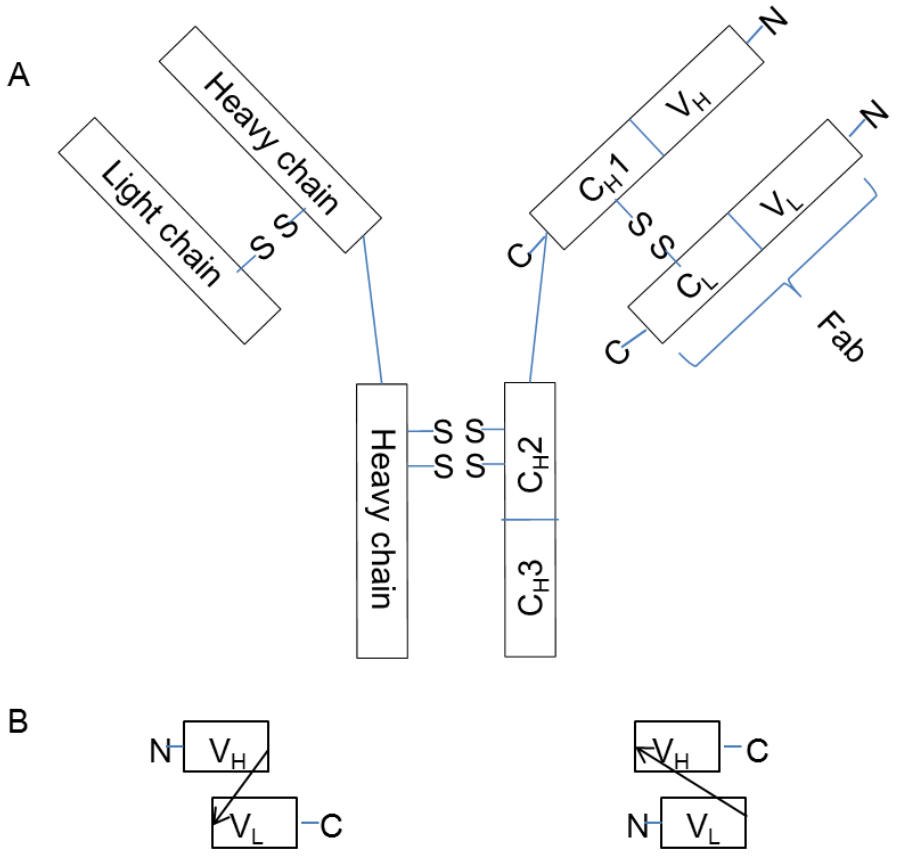

Figure 1.2 Antibody structures. (A) Linear structures of IgG and Fab (Wang et al., 2006); **(B)** Structure of scFv (Peterson et al., 2008).

Phage display is a method widely used for study of interactions between proteins by displaying library proteins on bacteriophages' coat and selecting the ones can bind to the target molecules like proteins, peptides or DNAs (Smith, 1985). In phage antibody display, antibody genes are cloned at the N-terminal of coat protein pIII, and expressed and displayed as fusion proteins with the coat protein pIII of filamentous bacteriophage (Smith and Petrenko, 1997). Then phage library carrying different antibody genes can be screened against the target molecules to select the clones binding to the antigen. This

technique can achieve to select and enrich antigen specific antibodies from large libraries in vitro (Hoogenboom et al., 1991; Hoogenboom, 2005).

In the antibody yeast surface display system, antibodies are usually expressed in their scFv format and fused to the subunit of the yeast agglutinin protein Aga2p, which binds to the Aga1p at the yeast cell wall through disulfide bonds. In this way, scFv is connected to the yeast cell wall (Chao et al., 2006). As a special application of flow cytometry, fluorescence-activated cell sorting (FACS) has been developed for high speed (>10,000 events per second) sorting a heterogeneous mixture of cells based on light scattering and fluorescent characteristics of individual cells (Bonner et al., 1972). The yeast cells displaying antibodies at their surface can be labeled with different fluorescence dye conjugated molecules like antigens, antibodies, inhibitors or peptides, and sorted by FACS according to desired fluorescence characters (Feldhaus et al., 2003).

MMP-14 inhibitory antibodies need both specificity and inhibition for not only binding to MMP-14 but also inhibiting the enzyme activities. This implies that the inhibitory antibody needs to bind to specific surface (epitope) on antigen MMP-14, i.e. to cover the enzyme active site of MMP-14 (Nam and Ge, 2013; Fernandez-Catalan et al., 1998). However, phage display and selection technique rely on binding thus can only provide the affinity information (Hoogenboom et al., 1991). In this study, we aim to overcome this technique handicap by developing a dual color FACS method, which can select specific MMP-14 antibody inhibiting MMP-14's enzymatic activity. This development is based on the interaction between MMP-14 and its native inhibitor TIMP-

2. We plan to conjugate MMP-14 and its inhibitor N-TIMP-2 with fluorescence Alexa 488 and Alexa 647 respectively then followed by dual color sorting to distinguish inhibitory antibodies from non-specific or non-inhibitory clones (**Figure 3.13** in **Results** for details).

1.4 Principle and applications of FACS

FACS provides rapid, objective and quantitative detection of fluorescent signals from individual cells as well as distinct separation of cells according to their particular differences. The first cell sorter was invented by Mack Fulwyler in 1965, following the Coulter principle, but it is very difficult and no longer used now. The technology was improved by Len Herzenberg, who was the first to use the term FACS, and won the Kyoto Prize in 2006 for his outstanding contributions in flow cytometry (Julius et al., 1972).

As for the principle, after the cell sample suspension is injected through the inner nozzle, cell-free sheath fluid flows around the inner nozzle to accelerate and narrow the cell inner stream. The stream is illuminated immediately by an argon laser which has been changed to proper value of wavelengths, and a vibrating mechanism divides the stream into individual droplets, which confirms one cell per droplet. When a cell crosses the laser beam and is illuminated for several microseconds, it will emit a fluorescent pulse and the signal pulse is shown at the photomultiplier output (Bonner et al., 1972). If the signal pulse from a cell is within predetermined amplitude limits, a charging pulse is generated electronically, and makes the cell contain the electrode. After being selectively

charged in this way, the droplet stream passes through an electrostatic field, and charged droplets are deflected by a distance proportional to their charge strengths. Thus the movements of different-charged and uncharged drops are separated, and are collected in separate collecting tubes (Bonner et al., 1972; Herzenberg et al., 2002).

FACS has a lot of applications, which are mainly involved in the quantifying and identifying single cell phenotype, bacteria cell expression, and isolating the specific cells (Herzenberg et al., 2002; Becker et al., 2004). One of the earliest applications is the analysis of functional distinctions between human peripheral blood cells (Herzenberg et al., 2002). For example, people used FACS to study the cytokine production of individual T-cell CD4 subsets, exploited markers to stain the cytokines and distinct its subsets MT_1 and MT_2 by FACS according to their staining differences (Mitra et al., 1999). Except the traditional study of eukaryotic cell populations, FACS can also be used to detect single DNA molecules and surface-expressed protein situations of the bacteria cells (Fu et al., 1999; Cormack et al., 1996; Feldhaus et al., 2003). For surface protein cells, the surface expressed green fluorescent protein (GFP) was abundant in the cell expression detection field by FACS (Cormack et al., 1996). Besides, because monoclonal antibodies have high specificity to the antigens and can be easily conjugated or incorporated with fluorochromes, they have been widely used as FACS reagent markers (Parks et al., 1979; Herzenberg et al., 2002). With the help of these labeling antibodies, FACS could also be used to analyze the surface protein expression and secreted molecule situations of the bacteria cell systems which have no direct fluorescence, like *E.coli* surface display, yeast surface display, etc (Francisco et al., 1993; Boder et al., 1997). In our study, FACS is

used to analyze the surface antibody binding characters combined with yeast surface display system.

1.5 Yeast antibody surface display

Yeast, as a unique eukaryotic host, has the characteristics of post-translational modification for protein and convenience of gene library construction and selection. Thus yeast surface display provides one of direct protein display platforms for engineering mammalian proteins, like antibodies, ligands, receptors and inhibitors (Boder and Wittrup, 1997). Yeast surface display is a good method for isolating and engineering antibodies, which utilizes its affinity, specificity and stability for selection against various antigen targets, including T cell receptors (Kieke et al., 1999), carcinoembryonic antigen (Graff et al., 2004), etc. Also this method can select the stable or fluorescence protein, like thermo stable proteins (Shusta et al., 1999) and GFP (Huang and Shusta, 2005).

In the antibody yeast surface display system, antibodies are expressed as a scFv format, which is fused to the adhesion subunit of the yeast agglutinin protein Aga2p, which can bind to the Aga1p by disulfide bonds to attach to the yeast cell walls (**Figure 1.3**) (Chao et al., 2006). The vector is pCTCON-2 (**Figure 2.1** in **Materials and Methods**, Page 20) which contains different function gene parts. *GAL1* promoter is used to induce the expression of protein Aga2p scFv fusion, and *TRP1* is used for selection in *Saccharomyces cerevisiae.* Ampicillin resistance gene and pUC origin are used for selection and replication in *E.coli* respectively. Aga1p gene is integrated into the chromosome gene after galactose-inducible promoter, which is why Aga1p and Aga2p

can be expressed at the same time (**Figure 1.3**) (Boder and Wittrup, 1997; Chao et al., 2006).

Combined with FACS, yeast surface display is good for the protein directed evolution, which realizes the quantitative screening, single cell identification and isolation, achieving the equilibrium activity and statistics of the samples to be observed directly during the cell screening process (Feldhaus et al., 2003). As FACS can detect multi-properties of the cell surface through multiple fluorescence labeling technique, multiple parameters can be controlled and observed together in one chart of a kind of cells. For example, the dual color FACS yeast antibody display is widely used for both expression and binding test, and people labeled the expressed cells with anti-c-Myc IgY/ Alexa Fluor 488-conjugated goat anti-chicken IgG for expression detection and biotinylated antigen followed by streptavidin-phycoerythrin (PE) for antigen binding, then an appropriate sorting gate was marked in the double-positive quadrant to isolate cells that were positive for both scFv expression and antigen binding (Boder and Wittrup, 1997; Chao et al., 2006). In our project, utilizing the character of multi-fluorescence scanning, after labeling the expressed cells with fluorescence antigen Alexa 488-MMP-14 and fluorescence inhibitor Alexa 647-N-TIMP-2, the MMP-14 antibodies affinity and inhibition can be identified respectively.

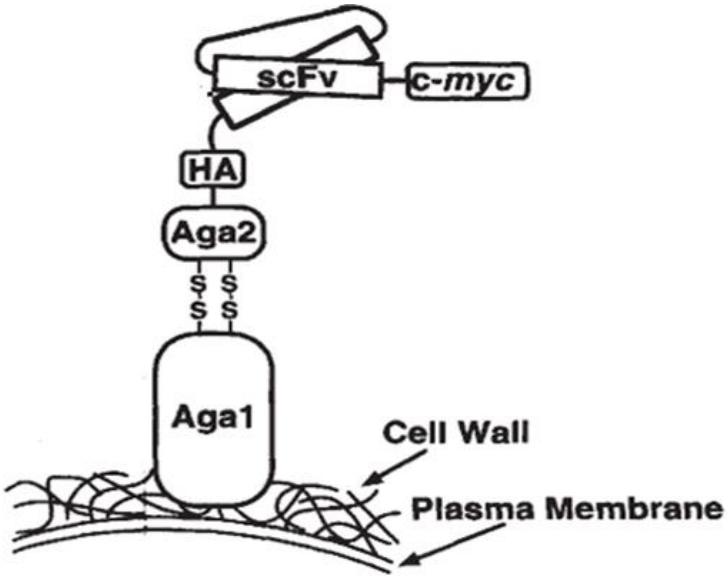

Figure 1.3 Yeast scFv surface display (Chao et al., 2006).

1.6 Objectives

We aim to develop a method to select inhibitory antibodies by FACS, which will be achieved by labeling the target MMP-14 (matrix metalloproteinase 14) with fluorophore Alexa 488 and its native inhibitor TIMP-2 (Tissue inhibitor of metalloproteinase 2) with fluorophore Alexa 647, and then followed by dual color FACS scanning of yeast cells on which the control scFv antibodies were surface displayed.

More specifically, we aim to achieve the following tasks: (1) Produce the catalytic domain of MMP-14; (2) Produce the N-terminal domain of TIMP-2; (3) Conjugate MMP-14 and N-TIMP-2 with fluorescence Alexa 488 and Alexa 647 respectively; (4) Convert several antibody clones to their scFv formats and clone them into the yeast display vector; (5) Identify MMP-14 specific clones from non-specific clones; (6) Distinguish inhibitory antibodies from non-specific or non-inhibitory antibodies.

2 Materials and Methods

2.1 MMP-14 expression, purification and refolding

The catalytic domain of MMP-14 with its hinge region (chMMP-14) was cloned into pET32b (Novagen, Madison, WI) as described in our previous study (Nam and Ge, 2013). *E.coli* BL21 (DE3) transformed with pET32b-chMMP-14 was cultured in LB medium to reach 0.8-1.0 OD_{600}, then isopropyl-β-D-thiogactopyranoside (IPTG) was added to a final concentration of 1 mM to induce chMMP-14 expression at 37 ℃ for 6 h. The cells were harvested by centrifugation at 5,000 ×g for 10 min then resuspended in 1/10 culture volume of 50 mM Tris-HCl (pH 8.0), 100 mg/mL of lysozyme and 0.1% of Triton X-100. After incubation at 30 ℃ for 15 min, cells were lysed by sonication and clarified by centrifugation at 10,000 ×g 4 ℃ for 25 min. Pellets were resuspended in solubilization buffer containing 6 M urea, 50 mM Tris-HCl (pH 8.0) and 30 mM 2-mercaptoethanol. The denatured protein solution was loaded onto a column filled with 1 mL of Ni^{2+}-NTA affinity resin (Qiagen, Valencia, CA). After washing with 10 mL of solubilization buffer supplemented with 20 mM imidazole, chMMP-14 was eluted by 6 M urea, 50 mM Tris-HCl (pH 8.0) and 200 mM imidazole. The collected chMMP-14 fractions were diluted to 30 mg/mL in 50 mM Tris-HCl (pH 8.0), 6 M Urea and 150 mM 2-mercaptoehanol, and dialyzed against 6 L of 50 mM Tris-HCl (pH 7.5), 150 mM NaCl, 5 mM $CaCl_2$, and 0.5 mM $ZnCl_2$ at 4 ℃ for 24 h.

2.2 N-TIMP-2 cloning, expression, purification and refolding

DNA fragment encoding the N-terminal domain of tissue inhibitors of metalloproteinases 2 (N-TIMP-2) was assembled from 12 synthetic oligonucleotides

(primer 1-primer 12, **Table 2.1**) and amplified by PCR using primer 1 and primer 12 (**Table 2.1**). Assembled N-TIMP-2 gene was cloned into NdeI/XhoI sites of pET32b，and obtained plasmid pET-N-TIMP-2 was transformed into *E.coli* BL21 (DE3) cells. The expression and purification procedures of N-TIMP-2 were similar to those of chMMP-14 with differences in the solubilization buffer (6 M GdnHCl, 50 mM Tris-HCl (pH 8.0) and 10 mM DDT) and the Ni^{2+}-NTA affinity column washing buffer (6 M GdnHCl, 50 mM Tris-HCl (pH 8.0), 10 mM DDT and 20 mM imidazole). After Ni^{2+}-NTA affinity column purification, N-TIMP-2 was diluted to 50 mg/mL in 50 mM Tris-HCl (pH 8.8), 1.5 M GdnHCl, 0.3 mM reduced glutathione and 0.5 mM oxidized glutathione, and was incubated at 4 ℃ overnight. The obtained protein solution was then dialyzed against 2 L of 50 mM Tris-HCl (pH 7.5) at 4 ℃ for 8 h.

2.3 MMP-14 and N-TIMP-2 assay

The chMMP-14 activity was measured using a fluorogenic substrate peptide 5-FAM/QXL™520 (AnaSpec, San Jose, CA) which has a MMP-14 recognition site between a pair of fluorophore-donor and quencher-acceptor. The assays were performed using 96-well plates in 50 mM Tris-HCl (pH 7.5), 150 mM NaCl, 5 mM $CaCl_2$ and 0.5 mM $ZnCl_2$, with 1-7 nM MMP-14 and 15-8000 nM substrate. Substrate cleavage was monitored at excitation/emission wavelengths of 490 nm/520 nm at 37 ℃ for 60 min in a Synergy^{TM} microplate reader (BioTek, VT).

N-TIMP-2 inhibition was tested using 0-3 μM N-TIMP-2 and 2 nM chMMP-14. In reaction buffer (the same buffer as MMP-14 assay), MMP-14 and N-TIMP-2 were

well mixed and incubated at room temperature for 20 min, then peptide substrate 5-FAM/QXL™520 was added to the final concentration of 1 μM. Relative fluorescence units (RFU) overtime were measured to obtain the reaction rates for different N-TIMP-2 concentrations (0-2 μM). Inhibition percentages were calculated using Equation 1. The correlations between the inhibition percentages and N-TIMP-2 concentrations were plotted using Origin (Origin Lab, CA) and the IC_{50} was estimated using the plots.

$$\text{Inhibiton percentage for x nM TIMP2} = 1 - \frac{\text{Cleave rate with x nM of TIMP2}}{\text{Cleave rate with 0 nM of TIMP2}} \qquad \text{(Eq.1)}$$

2.4 Fluorescence labeling of MMP-14 and N-TIMP-2

Alexa Flour® protein labeling kits (Invitrogen, CA) were used to conjugate chMMP-14 with Alexa 488 and N-TIMP-2 with Alexa 647 respectively following manufacture's manuals. Briefly, purified MMP-14 was concentrated using Amicon Ultra-15 Centrifugal Filter Units (EMD Millipore, MA) to be > 1 mg/mL, then dialyzed against conjugation buffer 25 mM HEPES (pH 7.5), 150 mM NaCl, 5 mM $CaCl_2$, and 0.5 mM $ZnCl_2$. 100 μl of 1.8 mg/ml MMP-14 solution was added to the reaction tube, and mixed with 10 μl of 1 M freshly prepared sodium bicarbonate. One vial of Alexa Fluor 488 TFP ester was completely dissolved in 10 μl dH_2O, and 2 μl of which was transferred to the reaction tube. After mixing thoroughly, the reaction tube was incubated at room temperature in dark for 15 min. To purify Alexa 488-MMP-14 conjugates, size exclusion columns (Mini UNOsphere, Bio-rad, CA) were first prepared by washing 5 times with 800 μl conjugation buffer. 50 μl conjugation solution was then loaded onto each column and centrifuged at 1,000 ×g for 1 min to isolate labeled MMP-14 from unconjugated dye.

Collected Alexa 488-MMP-14 was dialyzed against the 50 mM Tris-HCl (pH 7.5), 150 mM NaCl, 5 mM $CaCl_2$ and 0.5 mM $ZnCl_2$ at 4 ℃ for 8 h. Because Alexa 488 has its maximum excitation wavelength at 365 nm, Alexa 488 conjugated MMP-14 can show fluorescence under ultraviolet (UV) light. To track the conjugation process, MMP-14 samples before and after conjugation, and after purification of conjugated protein, were subjected to SDS-PAGE, which was observed under 365 nm UV light then stained with coomassie blue. The similar procedures were applied to conjugate N-TIMP-2 using Alexa 647 NHS ester protein labeling kit (Invitrogen, CA). Obtained MMP-14 and N-TIMP-2 Alexa conjugates were stored at -80 ℃. The degrees of labeling (DOL) for Alexa 488-MMP-14 and Alexa 647-N-TIMP-2 were calculated using Equation 3-5 and Equation 6-8 respectively. The A_{280} at 1 mg/mL for MMP-14 and N-TIMP-2 were obtained by Protein Calculator v3.4 (http://protcalc.sourceforge.net/).

$$\text{Protein concentration (mg/mL)} = \frac{(\text{A280-0.11} \times \text{A494}) \times \text{dilution factor}}{\text{A280 of protein at 1 mg/mL}} \quad \text{(Eq. 2)}$$

$$\text{Protein concentration (M)} = \frac{\text{protein concentration (mg/mL)}}{21{,}000} \quad \text{(Eq. 3)}$$

$$\text{DOL=(moles dye)/ (mole protein)} = \frac{\text{A494} \times \text{dilution factor}}{71{,}000 \times \text{protein concentration (M)}} \quad \text{(Eq. 4)}$$

$$\text{Protein concentration (mg/mL)} = \frac{(\text{A280-0.03} \times \text{A650}) \times \text{dilution factor}}{\text{A280 of protein at 1 mg/mL}} \quad \text{(Eq. 5)}$$

$$\text{Protein concentration (M)} = \frac{\text{protein concentration (mg/mL)}}{14{,}700} \quad \text{(Eq. 6)}$$

$$\text{DOL=(moles dye)/ (mole protein)} = \frac{\text{A650} \times \text{dilution factor}}{239{,}000 \times \text{protein concentration (M)}} \quad \text{(Eq. 7)}$$

Table 2.1 Sequences of oligonucleotide primers for molecular clonings

#	Function	Sequence
1	N-TIMP-2 assembly	5'-GCGTAGCATATGTGTAGCTGCAGTCC-3'
2	N-TIMP-2 assembly	5'-CAATATCGGCATTGCAAAACGCCTGCTGCGGATGCACCGGACTGCAGCTACACATATG-3'
3	N-TIMP-2 assembly	5'-GCGTTTTGCAATGCCGATATTGTGATTCGTGCGAAAGCGGTGAACAAAAAGGAAGTGG-3'
4	N-TIMP-2 assembly	5'-GTTTAATCGGATTGCCATAGATATCGTTGCCGCTATCCACTTCCTTTTTGTTCACCGC-3'
5	N-TIMP-2 assembly	5'-ACGATATCTATGGCAATCCGATTAAACGTATTCAGTATGAAATAAAGCAGATCAAAAT-3'
6	N-TIMP-2 assembly	5'-TCAATGTCCTGATCCGGGCCTTTAAACATTTTGATCTGCTTTATTTCATACTGAATAC-3'
7	N-TIMP-2 assembly	5'-GCCCGGATCAGGACATTGAGTTCATTTATACCGCACCGGCAGCAGCGGTGRGCGGCGT-3'
8	N-TIMP-2 assembly	5'-GCCCGCAATCAGATATTCTTTTTTGCCGCCATTATCCAGGCTCACGCCGCACACCGCT-3
9	N-TIMP-2 assembly	5'-CAAAAAAGAATATCTGATTGCGGGCAAAGCGGAAGGCAATGGCAACATGCACATAACC-3'
10	N-TIMP-2 assembly	5'-GCTCAGGGTATCCCACGGCACAATGAAATCGCACAGGGTTATGTGCATGTTGCCATTG-3'
11	N-TIMP-2 assembly	5'-GCCGTGGGATACCCTGAGCGCGACCCAGAAAAAAAGCCTGAATCATCGTTATCAGATG-3'
12	N-TIMP-2 assembly	5'-GCTAGCTCGAGGCAGCCCATCTGATA-3'
13	DX-2400 forward	5'-GCGCGCTAGCGAAGTGCAGCTGCTGGAATCTGG-3'
14	DX-2400 reverse	5'-CGGGTCTCGGATCCTTTGATATCTACTTTAGTGCCCGGACC-3'
15	M18 forward	5'-GCGCGCGCTAGCGATATTCAGATGACACAGACTACATCC-3'
16	M18 reverse	5'-CGGGTCTCGGATCCCGAGGCCGAGGAGACGGTGAC-3'
17	b12 forward	5'-GCGCGCTAGCCAAGTACAGCTGGTACAGTCTGG-3'
18	b12 reverse	5'-GCGCGGATCCACGTTTACGTTCCAGTTTGGTACCC-3'
19	VH forward	5'-CGCTGGGCCCAGCCGGCCAT-3'
20	VH reverse	5'-AGAGCCACCTCCGCCTGAACC-3'
21	VL forward	5'-GGCGGAGGTGGCTCTGGCGG-3'
22	VL reverse	5'-CGCTGGGCCCCCGAGGCCCC-3'
23	scFv forward	5'-GCGCGCTAGCGAAGTTCAGCTGCTGGAATCTGG-3'
24	scFv reverse	5'-GCGCGGATCCTCGCTTGATCTCAAGCTTGGTACC-3'

2.5 Antibody yeast surface display

The Fab genes of 1F8, 2A10, 3B1, 1H11, 2D9, 2F9 and 1B11 were modified to their scFv formats for yeast surface display. For each antibody clone, V_H fragment was amplified by PCR using primer 19 and 20, and V_L fragment was amplified using primer

21 and 22 (**Table 2.1**). Amplified V_H and V_L fragments were assembled by overlapping PCR using primer 23 and primer 24. The scFv genes of DX-2400, M18 and b12 antibodies were amplified from pMoPac-DX2400, pMoPac-M18 and pMoPac-b12 as the templates by PCR using primer 13-18 (**Table 2.1**). Obtained scFv genes were cloned into NheI/BamHI sites of yeast surface display plasmid pCTCON-2 (**Figure 2.1**), which has Aga2p protein at N-terminal for surface anchoring and a c-Myc tag at C-terminal for detection. The resulting antibody display plasmids were transformed into yeast EBY100 cells by EZ transformation II kit (Zymo Research, CA), and cells were selected on SDCAA plates at 30 ℃ overnight. The SDCAA medium contains 5 g/L casamino acids, 20 g/L dextrose, 1.7 g/L YNB (Yeast Nitrogen Base without ammonium sulfate amino acids), 10.19 g/L Na_2HPO_4-$7H_2O$, and 8.56 g/L NaH_2PO_4-H_2O. For each antibody clone, a single yeast colony was picked to inoculate into 5 mL SDCAA medium and cultured overnight at 30 ℃ and 225 rpm. When the culture reached 4 OD_{600}, the cells were centrifuged at 3000 ×g for 5 min. After the supernatant was discarded, the cell pellets were resuspended in 20 mL SGCAA medium, which was similar to SDCAA medium except 20 g/L galactose instead of 20 g/L dextrose was used. The cells were continuously cultured at 25 ℃ and 225 rpm for 48 h for antibody expression and display.

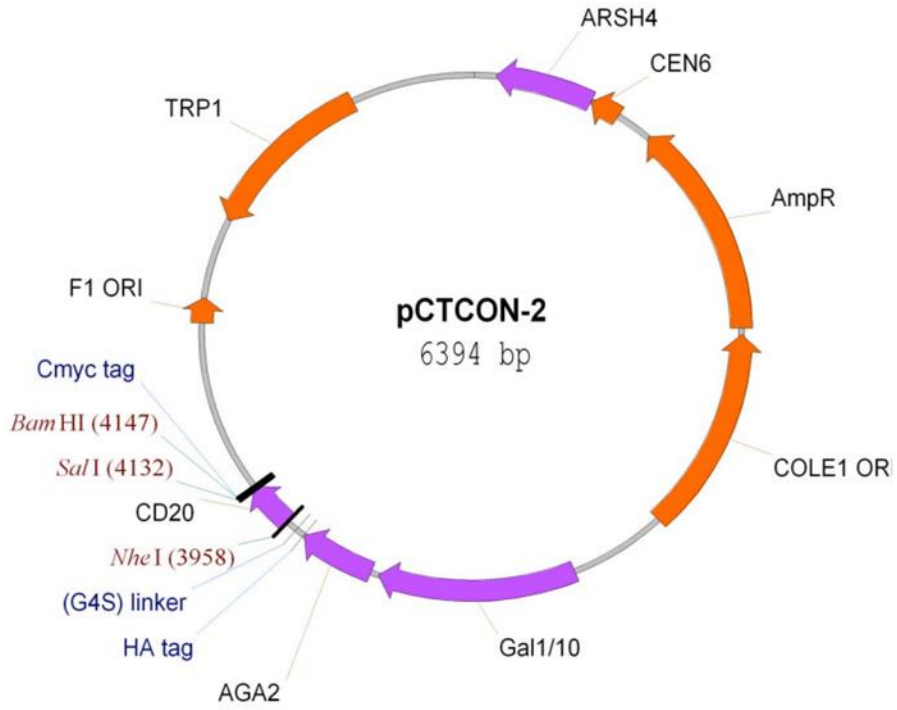

Figure 2.1 Plasmid map of pCTCON-2 (Chao et al., 2006).

2.6 ELISA for antibody surface display

4 OD_{600} cells of different antibody clones, CD20 and untransformed clones were centrifuged at 5,000 ×g for 5 min to harvest the cells. The cell pellets were resuspended in 200 µl PBS supplemented with anti-c-Myc antibody 9E10 conjugated with HRP (Santa Cruz Biotechnology, CA) at 1:1000 dilution. The cells were incubated with shaking at room temperature for 1 h, then centrifuged at 3,000 ×g for 5 min. After washing 5 times with 2 mL PBST buffer (1× PBS, 0.05% Tween20), cell pellets were resuspended with 200 µl Onestep™ Ultra TMB-ELISA solution (Thermo Scientific, MA) and incubated at room temperature in the dark for 3 min. 200 µl H_2SO_4 was added to stop the reaction, and

mixtures were centrifuged at 17,000 ×g for 30 s. The absorbance of supernatant was measured at 450 nM using an Epoch microplate reader (BioTek, VT).

2.7 Fluorescent microscopy imaging

After induction for 48 hours, 0.1 OD_{600} DX-2400, M18, and CD20 cells were centrifuged and resuspended in MMP-14 buffer (50 mM Tris-HCl (pH 7.5), 150 mM NaCl, 5 mM $CaCl_2$, 0.5 mM $ZnCl_2$). The harvested cells were then incubated with 4 μg/mL of Alexa 488-MMP-14 at room temperature for 30 min and washed once with MMP-14 buffer. The images of cells labeled with Alexa-488-MMP-14 were observed by BX51-P polarizing microscope (Olympus, Japan) using the FITC filter (FITC and Alexa 488 share the same excitation and emission wavelengths). The objective lens and eyepiece lens have magnification/numerical aperture of 10× and 100× respectively.

2.8 Fluorescence scanning

For anti-c-Myc fluorescence scanning, 0.1 OD_{600} of antibody clones, CD20 and untransformed clones were harvested by centrifugation, and resuspended in 50 mM Tris-HCl (pH 7.5) and 150 mM NaCl. Primary chicken anti-c-Myc IgY (Invitrogen, CA) was added to cell suspensions at 1:500 dilution. After incubation with shaking at room temperature for 30 min, cells were centrifuged at 3,000 ×g for 5 min and washed once with 50 mM Tris-HCl (pH 7.5) and 150 mM NaCl. Secondary Alexa Fluor 647-goat anti-chicken IgG (Invitrogen, CA) was then added to cell suspensions at 1:100 dilution, and incubated with shaking on ice for 20 min. After washing once, the cells were resuspended in 500 μl 50 mM Tris-HCl (pH 7.5) and 150 mM NaCl. Using a FACSAria (BD) flow

cytometer, the excitation laser line of 633 nm was selected with voltage of 775, and SSC and FSC were set at 585 and 220 voltages respectively. Threshold values for FSC and SSC were set at 5000 and as default. The gate for live cells was selected in FSC/SSC dot plot diagram to exclude low FSC events, which were likely associated with cell debris and contamination particles. The threshold for fluorescence positive cells in antibody display samples was determined in Alexa 647 histogram, using untransformed cells as the negative controls. For different sample batches, excitation laser voltage was subjected to adjust if necessarily to distinguish antibody displayed cells from negative controls. Typically 10,000 events were recorded for FACS scanning of each sample.

For Alexa 488-MMP-14 and Alexa 647-N-TIMP-2 dual color labeling, 0.1 OD_{600} cells were centrifuged and resuspended in MMP-14 buffer (50 mM Tris-HCl (pH 7.5), 150 mM NaCl, 5 mM $CaCl_2$, 0.5 mM $ZnCl_2$). Cell suspensions were incubated with 4 μg/mL of Alexa 488-MMP-14 at room temperature for 30 min and washed once with MMP-14 buffer. Alexa 488-MMP-14 labeled cell suspensions were then incubated with 16 μg/mL of Alexa 647-N-TIMP-2 at 4 ℃ for 20 min. After washing once, cells were ready for scanning using FACSAria flow cytometer. The voltages of FSC and SSC and the gate for live cell events were set the same as anti-c-Myc fluorescence scanning. The excitation laser lines for the two fluorophores were 488 nm and 633 nm with voltages of 350-516 and 632-775 respectively. 10,000 events were recorded for each antibody clone. The fluorescence thresholds were adjusted using a positive control clone displaying DX-2400 scFv and negative control clones displaying non-relevant scFv antibodies (M18 and

b12) or non-specific scFv antibodies (2F9, 2D9, and 1B11) identified in our previous studies of phage panning (Nam et al., manuscript in preparation).

3 Results

3.1 Production of MMP-14

Catalytic domain of MMP-14 with its hinge region (chMMP-14) was produced in BL21 (DE3) cells under the control of a T7 promoter. After purification using Ni^{2+}-NTA column, ~4 mg of chMMP-14 can be typically obtained from 200 mL culture (**Figure 3.1,** Lane 2). Through the refolding process, the 24 kDa chMMP-14 was converted to a 22 kDa intermediate, then a 20 kDa mature format by autoproteolytic cleavage (**Figure 3.1**, Lane 4&5), a phenomenon in good agreements with previous studies (Koo, et al., 2002).

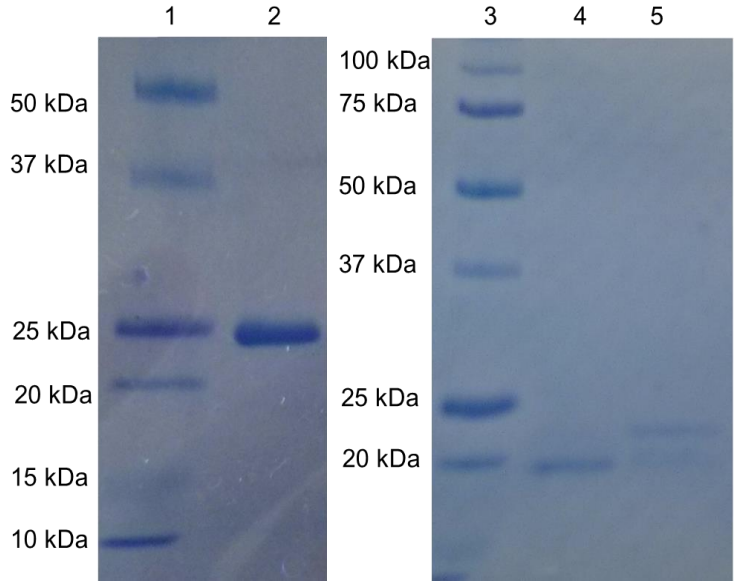

Figure 3.1 Production and refolding of chMMP-14. Lane 1&3, molecular weight ladders; Lane 2, purified chMMP-14; Lane 4, mature refolded chMMP-14; Lane 5, intermediate refolded chMMP-14.

To test the activity of refolded chMMP-14, FAM/QXL™520 was used as the substrate, in which QXL™520 quenched the fluorescence of 5-FAM. Upon cleavage into two separate fragments by MMP-14, the fluorescence of 5-FAM will be restored, and increases of relative fluorescence units (RFUs) can be monitored by a fluorescence microplate reader. When 2 nM chMMP-14 reacted with the substrate, RFUs increased over time indicating that refolded MMP-14 was active. As the concentration of substrate increased from 15 nM to 2 μM, the reaction rate increased (**Figure 3.2A**). The k_{cat} was calculated as 3.05×10^{-3}/sec, which was two orders of magnitudes slower than reported values (Lichte et al., 1996). K_M was measured as 660 nM by fitting with Michaelis-Menten model (**Figure 3.2B**) using the standard curve provided by the manufacture showing the relationship between RFU and concentration of cleaved product (**Figure 3.2C**). For conjugation, MMP-14 needed to present in HEPES buffer. Results of MMP-14 activity assays in Tris and HEPES buffers (**Figure 3.2D**) suggested that the specific activity of MMP-14 in HEPES was 82.9 ± 3.8% of that in Tris buffer (**Table 3.1**).

Table 3.1 Comparisons of MMP-14 activities in Tris and HEPES buffers.

	Activity in Tris (intensity/min)	Activity in HEPES (intensity/min)
149 nM MMP14	335	286
37.2 nM MMP14	115	92

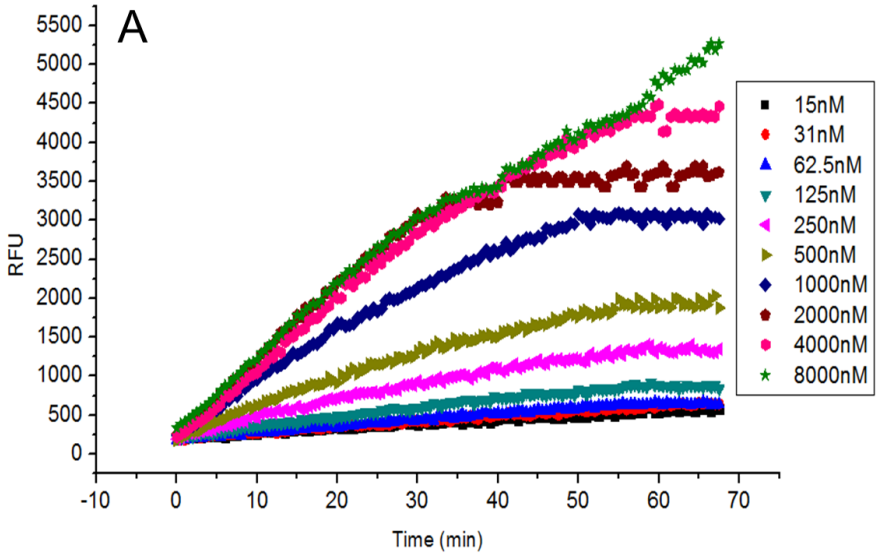
A
RFU
Time (min)
15nM
31nM
62.5nM
125nM
250nM
500nM
1000nM
2000nM
4000nM
8000nM

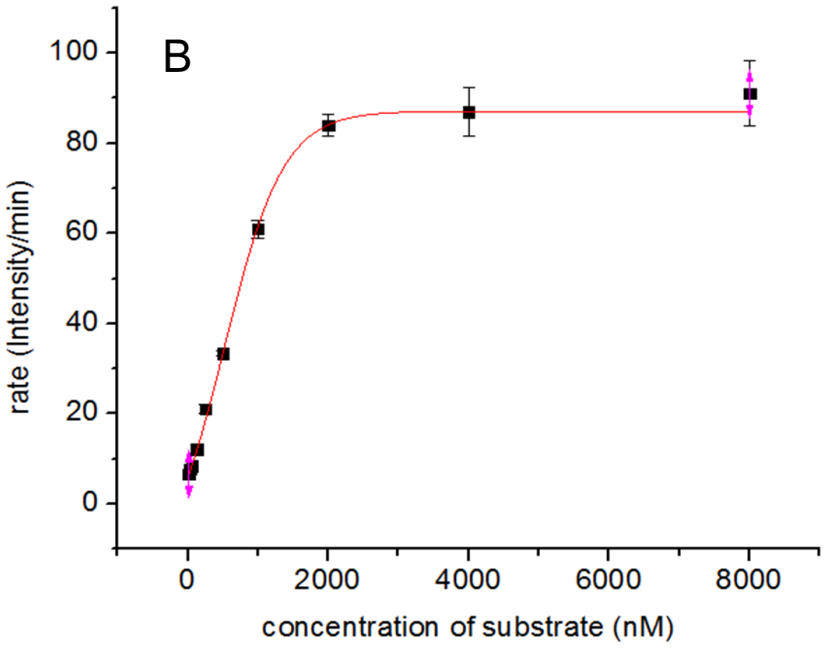
B
rate (Intensity/min)
concentration of substrate (nM)

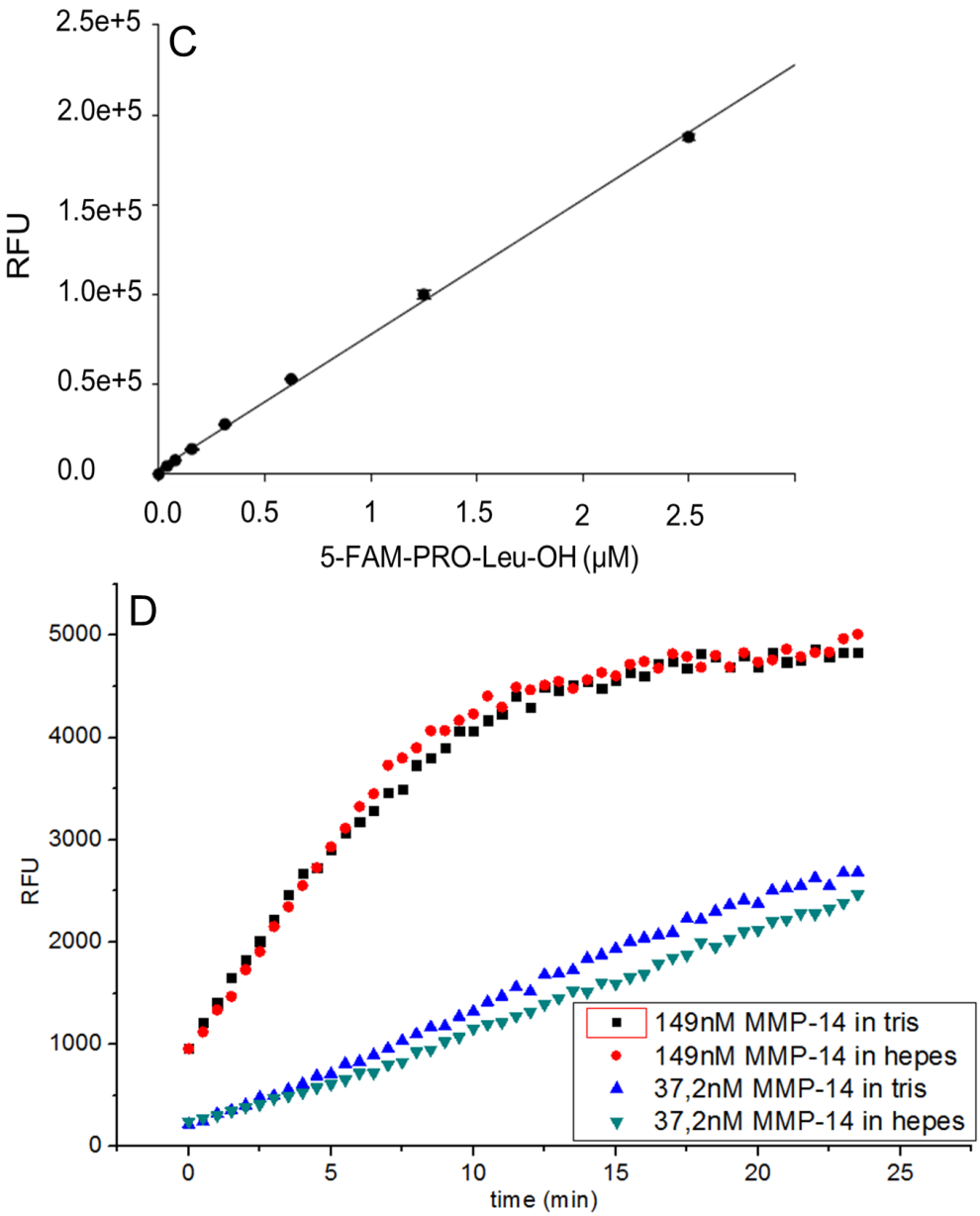

Figure 3.2 Activity assays of purified chMMP-14. (A) Plots of relative fluorescence units (RFUs) over time for cleavage of different concentrations of fluorogenic substrate peptide 5-FAM/QXL™520 by 2 nM chMMP-14. **(B)** Plot of reaction rates over substrate concentrations generated using Origin by fitting to Michaelis-Menten equation. **(C)** The standard curve of cleaved product (provided by the manufacture of substrate). **(D)** Comparisons of MMP-14 activities in Tris and HEPES buffers.

3.2 Production of N-TIMP-2

The 378 bp N-TIMP-2 gene was assembled and amplified by PCR (**Figure 3.3**, Lane 2) and cloned into plasmid pET32b to generate pET-N-TIMP-2. The resulting plasmid was tested by restriction enzyme digestion (**Figure 3.3**, Lane 4) and confirmed by DNA sequencing (**Appendix 1**). After induction using IPTG, SDS-PAGE analysis suggested that N-TIMP-2 was successfully expressed with its expected MW of ~15 kDa (**Figure 3.4**, Lane 2). After solubilized in 6 M GdnHCl and purified by the Ni^{2+}-NTA affinity column, ~5 mg N-TIMP-2 can be typically yielded from 200 mL of cell culture. SDS-PAGE analysis indicated that monomeric N-TIMP-2 was purified with a trace amount of N-TIMP-2 dimer (**Figure 3.4**, Lane 5). The purified N-TIMP-2 was then refolded and dialyzed, and SDS-PAGE results suggested majority of monomeric N-TIMP-2 was recovered with a lower amount of dimer (**Figure 3.4**, Lane 7).

For TIMP-2 inhibition assays, N-TIMP-2 and MMP-14 were incubated at RT for 20 min to form N-TIMP-2 / MMP-14 complex before addition of substrate. With increased N-TIMP-2 concentration, reaction rate decreased indicating that N-TIMP-2 inhibited MMP-14's activity (**Figure 3.5A**). Under the conditions of 2 nM MMP-14 and 1 μM substrate, 1.25 μM N-TIMP-2 completely inhibited MMP-14 activity. Inhibition percentages were calculated using Equation 1 in **Materials and Methods** (Page 16), and plotted against N-TIMP-2 concentration to obtain IC_{50} of ~25 nM (**Figure 3.5B**) for conditions of 2 nM MMP-14 and 1 μM substrate. Similarly, IC_{50}s for 0.3 μM, 0.6 μM, 1μM, 1.5 μM, 2 μM, 3.8 μM, and 4 μM substrate with 2 nM MMP-14 were also measured (**Table 3.2)**.

Because N-TIMP-2 is a competitive inhibitor of MMP-14, K_I was then calculated using Equation 8 to be 12.0 $\pm$ 8.3 nM in average.

$$K_I = \frac{IC_{50}}{1 + \frac{[S]}{K_M}} \quad \text{(Eq. 8)}$$

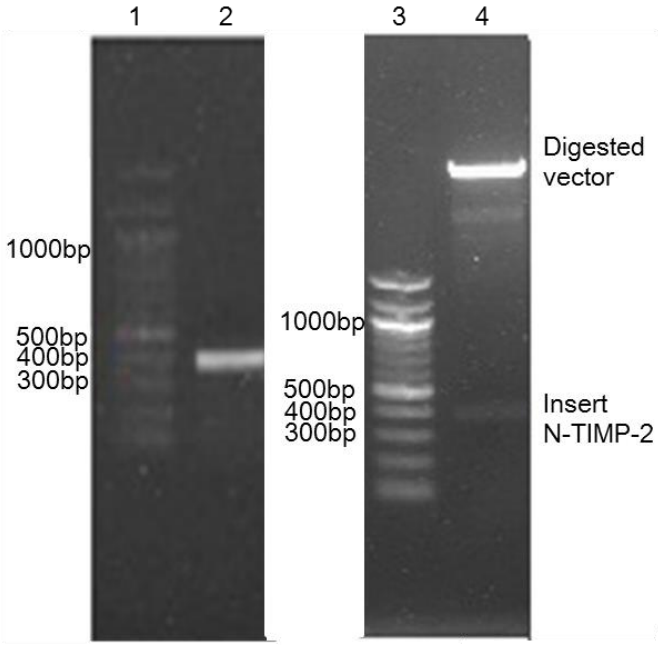

Figure 3.3 Cloning N-TIMP-2. Lane 1 & 3, DNA molecular weight ladders; Lane 2, PCR product of N-TIMP-2 gene (378bp); Lane 4, Digestion test of constructed pET-N-TIMP-2 with NdeI/XhoI showing fragment of N-TIMP-2 (~400bp) and vector (5.2k bp).

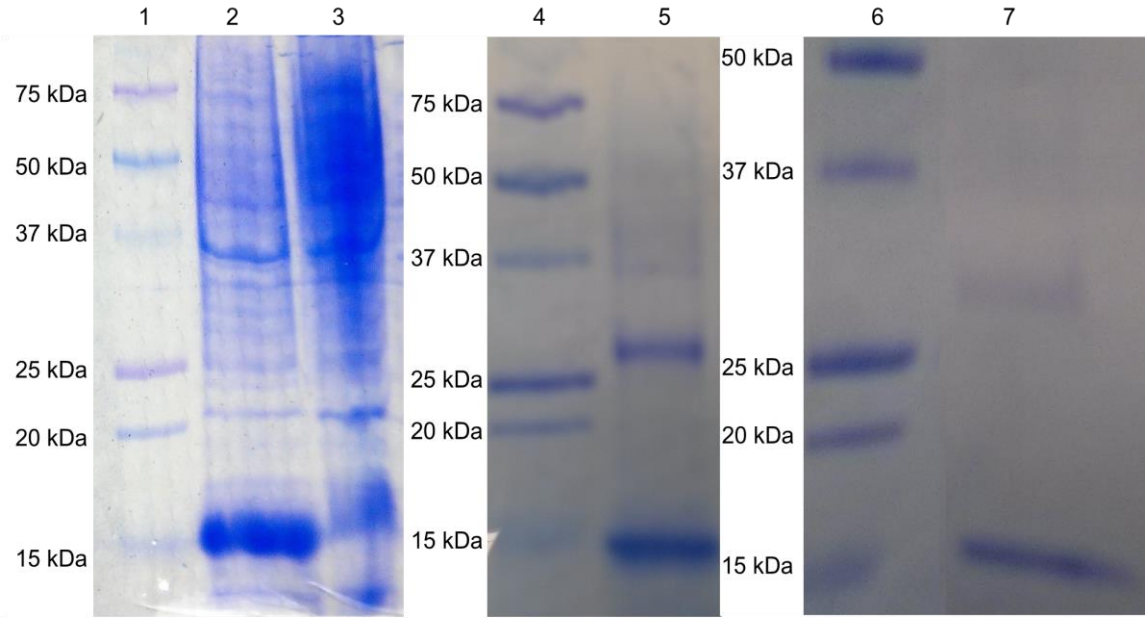

Figure 3.4 Expression, purification and refolding of recombinant N-TIMP-2. Lane 1, 4&6, molecular weight ladders. Lane 2, whole cell sample of induced culture; Lane3, whole cell sample of non-induced culture; Lane 5, purified N-TIMP-2; Lane 7, refolded N-TIMP-2.

Table 3.2 IC_{50}s for various concentrations of substrates.

Substrate concentration (μM)	IC_{50} (nM)	K_I (nM)
0.3	39.6	26.8
0.6	37.5	19.6
1.0	28.4	11.1
1.5	34.4	10.5
2.0	25.2	6.2
3.8	32.3	4.7
4.0	36.7	5.2

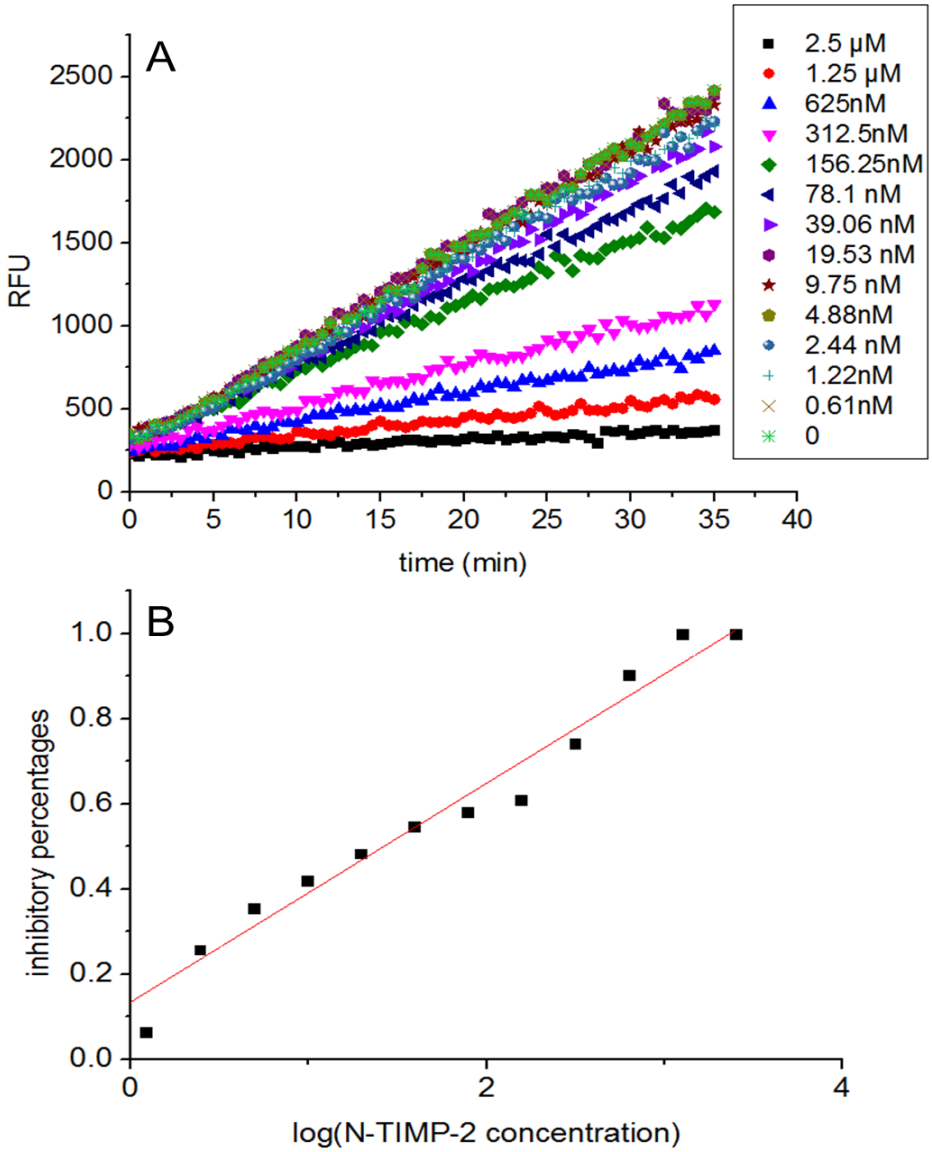

Figure 3.5 N-TIMP-2 inhibition assay. (A) Cleavage of 1 μM substrate by 2nM MMP-14 in different concentrations of N-TIMP-2 (0-2.5 μM). **(B)** Correlation between inhibition percentages and logarithms of N-TIMP-2 concentrations.

3.3 Fluorescence labeling of MMP-14 and N-TIMP-2

Concentrated MMP-14 and N-TIMP-2 were labeled using Alexa 488 TFP ester and Alexa 647 NHS ester respectively, through the crosslinking reactions between ester and primary amines on proteins (**Figure 3.6A**). X-Ray crystal structures of MMP-14 and TIMP-2 complex (PDB ID=1BQQ) suggested that there are multiple primary amine groups on their surfaces available for conjugations and most of these conjugation sites are distanced from the reaction pocket of MMP-14 (**Figure 3.6B**) or inhibition region on TIMP-2 (**Figure 3.6C**). After crosslinking reaction and purification to separate conjugated MMP-14 from unreacted dye, Alexa 488-MMP-14 samples were subjected to SDS-PAGE analysis. Under a UV lamp, conjugated samples showed fluorescent bands with an expected MW of 20 kDa. After purification using gel filtration centrifugation column, the amount of unconjugated dye was dramatically reduced (**Figure 3.7A**). Comparing to unconjugated MMP-14, obtained Alexa 488-MMP-14 conjugates remained its 88.7±2.3 % activity as shown in **Figure 3.7B**. And the degree of labeling (DOL) was calculated as 3.46 (**Table 3.3**) using Equation 2-4 in **Materials and Methods** (Page 17).

Table 3.3 Degrees of labeling (DOL) of MMP-14 and N-TIMP-2.

Protein	A_{280}	A_{494} or A_{650}	A_{280} at 1mg/mL by Protein calculator	Protein concentration (mg/mL)	Protein concentration (M)	DOL
MMP-14	0.289	1.12(A_{494})	1.73	0.0958	4.56×10^{-6}	3.46
N-TIMP-2	0.157	0.79(A_{650})	0.87	0.153	1.04×10^{-5}	0.32

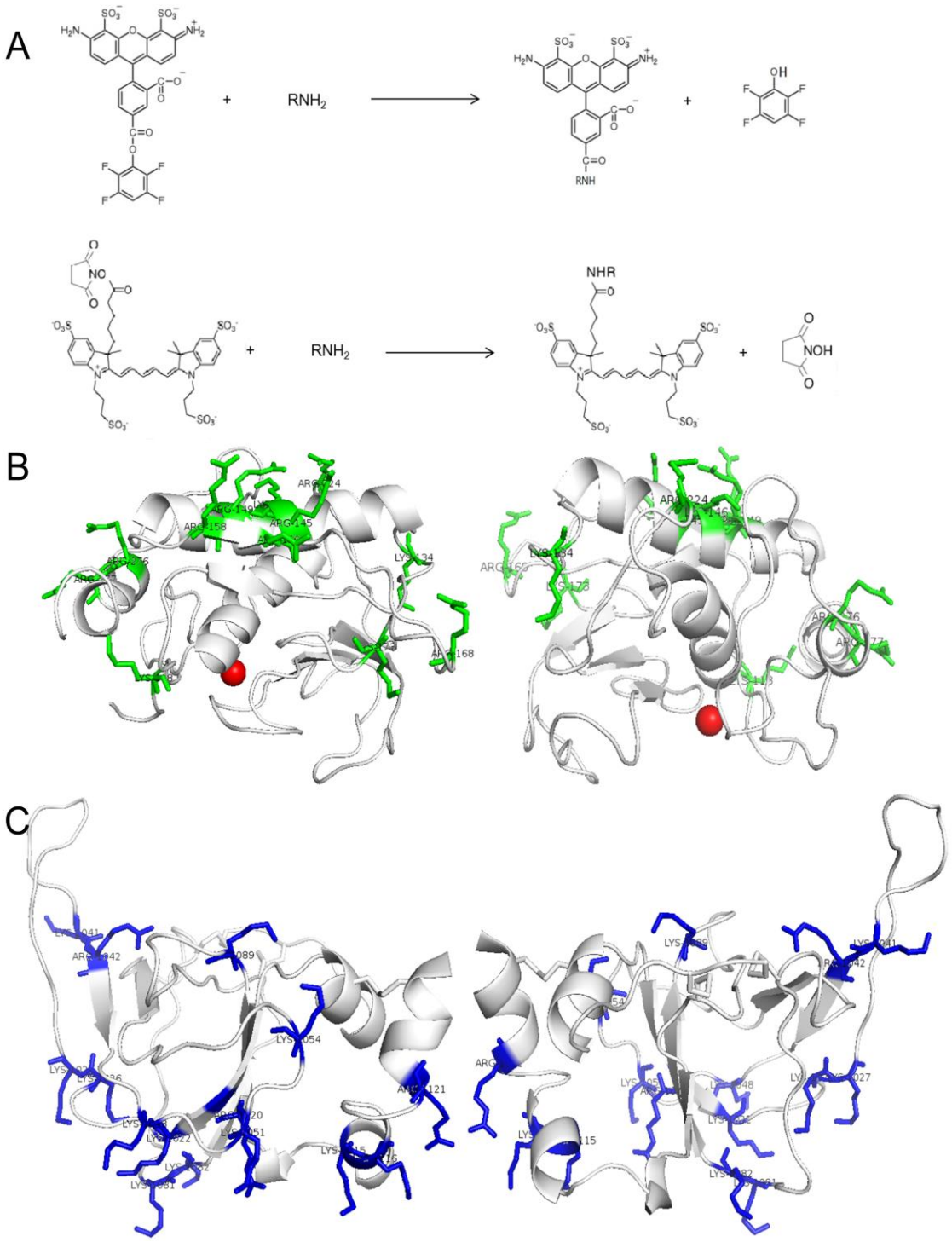

Figure 3.6 Mechanisms of crosslinking between ester groups and primary amines on proteins. (A) The reactions between the ester dye and primary amines; **(B)** Structure of MMP-14 with lysine and arginine residues highlighted; **(C)** Structure of TIMP-2 with lysine and arginine residues highlighted.

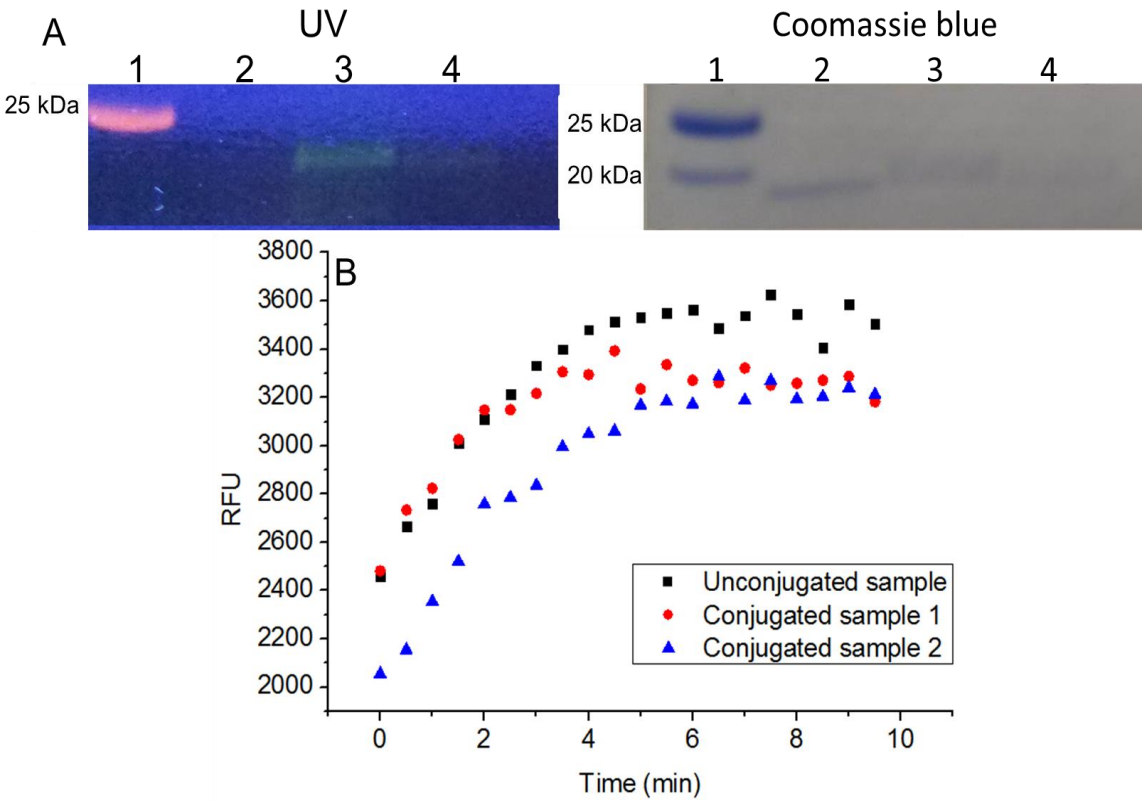

Figure 3.7 Conjugation of MMP-14 with Alexa 488. (A) SDS-PAGE analysis for conjugation process. Lane 1, protein molecular weight ladder; Lane 2, MMP-14 before conjugation; Lane3, MMP after conjugation; Lane 4, conjugated MMP-14 after purification. Left image, UV; right image, Coomassie blue. **(B)** Comparison of activities for conjugated and unconjugated MMP-14 (500 nM MMP-14, 1 μM substrate).

Similar procedures were applied for conjugating N-TIMP-2 with Alexa 647. SDS-PAGE analysis of unconjugated N-TIMP-2 and conjugated N-TIMP-2 before and after purification showed N-TIMP-2 bands with expected MW of 15 kDa (**Figure 3.8A**). The degree of labeling was calculated as 0.32 (**Table 3.3**) using Equation 5-7 in **Materials and Methods** (Page 17). The inhibition function of conjugated N-TIMP-2 was measured (**Figure 3.8B&C**) with an IC_{50} of 87.8 nM, which was ~2 folds higher than that of unconjugated N-TIMP-2 (**Figure 3.4**), indicating that conjugated N-TIMP-2 remained its inhibition function.

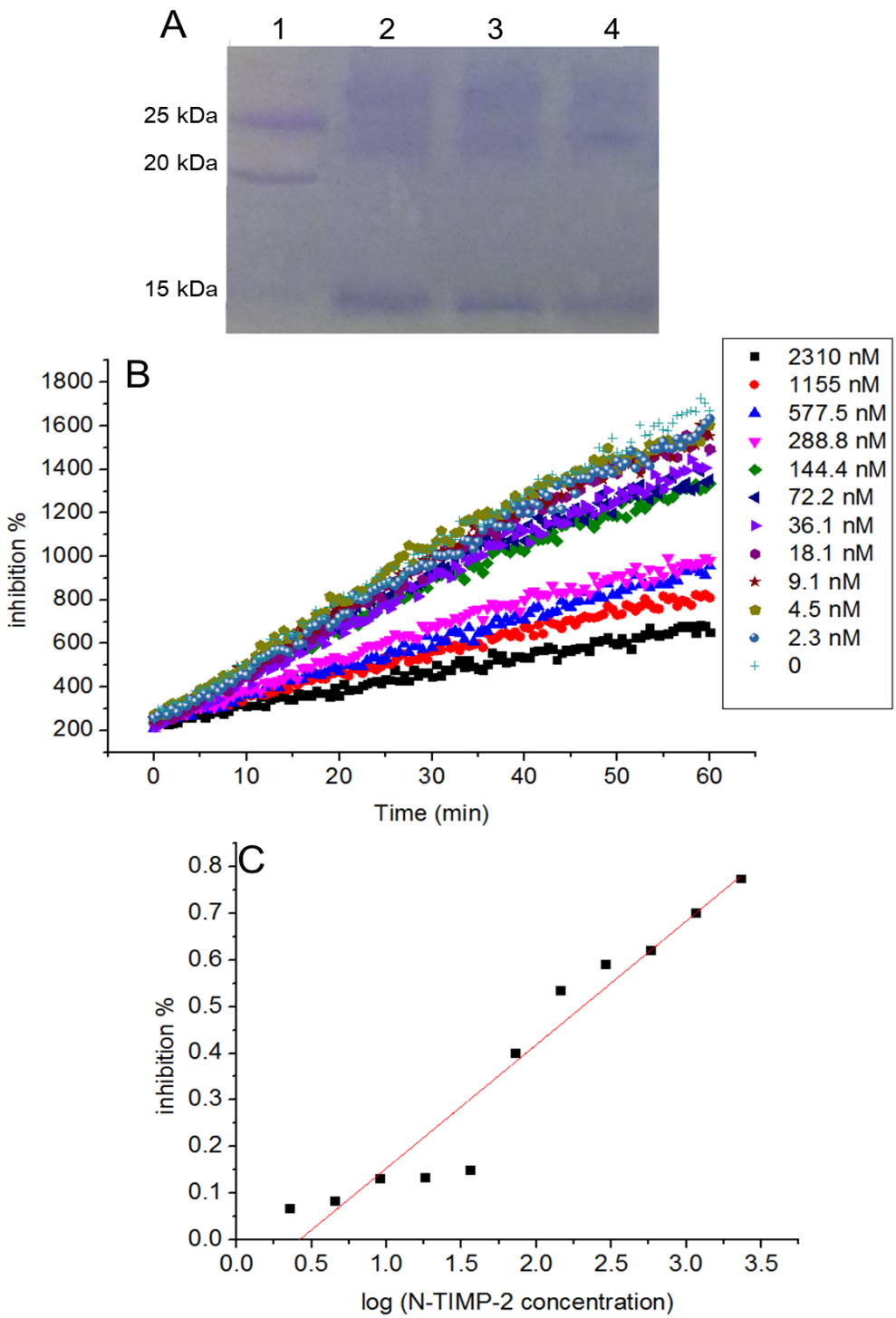

Figure 3.8 Conjugation of N-TIMP-2 with Alexa 647. (A) SDS-PAGE analysis of conjugation process. Lane 1, protein molecular weight ladder; Lane 2, unconjugated N-TIMP-2; Lane 3, conjugated N-TIMP-2 before purification; Lane 4, conjugated N-TIMP-2 after purification. **(B&C)** Inhibition assays of conjugated N-TIMP-2.

3.4 Antibody yeast surface display

The scFv antibodies of DX-2400, 1F8 and b12 were cloned and expressed on surface of EBY100 cells as described in **Materials and Methods** (Page 20). After being incubated with anti-c-Myc mAb 9E10 conjugated with HRP then TMB solution, DX-2400, 1F8 and b12 cell suspensions gradually turned blue, while the color of untransformed cell suspension (as the negative control) kept unchanged. After adding H_2SO_4, DX-2400, 1F8 and b12 cell suspensions turned yellow while the negative control did not change color (**Figure 3.9A**). After centrifugation, the supernatants of DX-2400, 1F8 and b12 samples had absorbance of ~0.5 OD at 450 nm, which was much higher than that of untransformed cells (~0.1 OD), indicating that DX-2400, 1F8 and b12 were successfully expressed and displayed on yeast cell surface (**Figure 3.9B**).

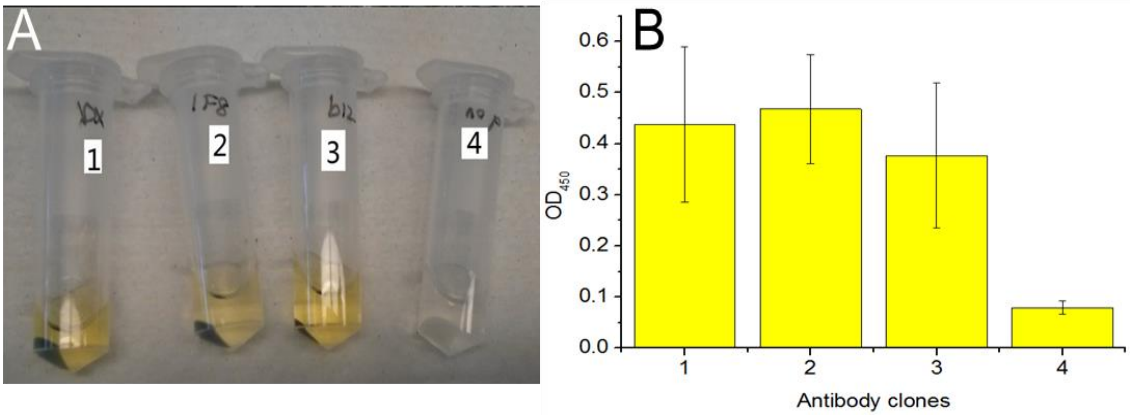

Figure 3.9 Cell ELISA results of antibody yeast surface display, using anti-c-Myc-HRP. (A) Photo. **(B)** Absorbance. 1, DX-2400; 2, 1F8; 3, b12; 4, untransformed.

The performance of antibody yeast surface display was further confirmed using FACS scanning for multiple antibody clones. In addition to above mentioned three scFvs (DX-2400, 1F8 and b12), M18 (anti-PA-63) and six scFv genes 2A10, 3B1, 1H11, 2D9, 2F9 and 1B11, which were previously isolated in our lab (Nam et at., manuscript in preparation), were cloned into pCTCON-2 for surface display tests. After incubation with the primary chicken anti-c-Myc IgY then the secondary Alexa Fluor 647-goat anti-chicken IgG, these scFv displaying cells were subjected for FACS scanning. Obtained Alexa 647 histograms (**Figure 3.10**) showed that all of these scFvs were successfully expressed on yeast cell surface at various levels with the florescence means (FM) ranging from 3.5×10^3 to 4.4×10^4, while the control cells without plasmid transformation had no detectable florescence signals (FM=1.5). Among these antibody clones, DX-2400 showed the highest FM of 43700 with 92% of cells are positive ($200 < FM < 2 \times 10^4$), and 2A10 showed the lowest FM of 3523 with 57% positive cells, and most of the antibody clones had FM of 10^4 and the average FM of the expressed clones was 1.7×10^4 with 79.7 ±10.2% positive cells in average.

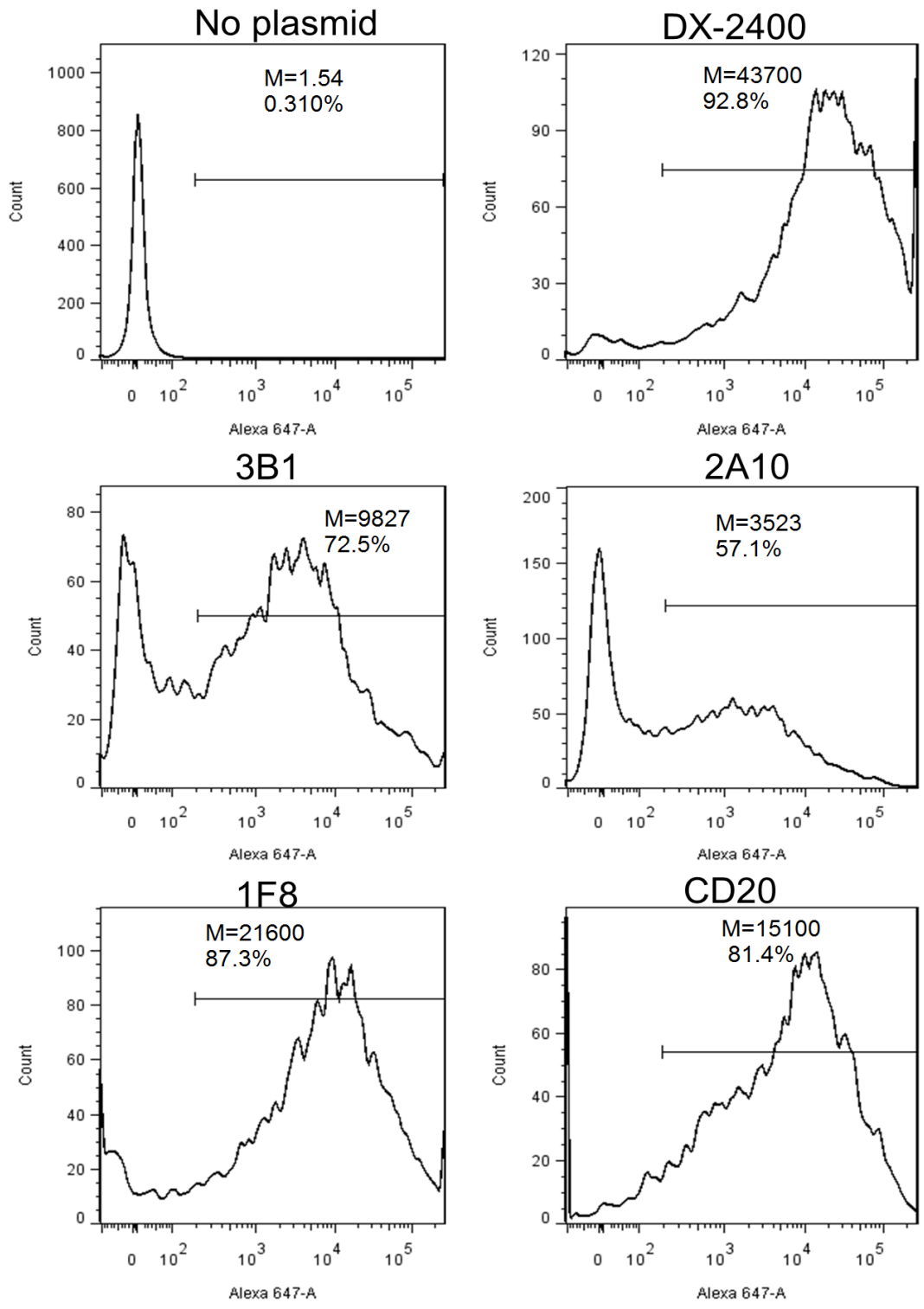
No plasmid
M=1.54
0.310%
DX-2400
M=43700
92.8%
3B1
M=9827
72.5%
2A10
M=3523
57.1%
1F8
M=21600
87.3%
CD20
M=15100
81.4%
Count
Alexa 647-A

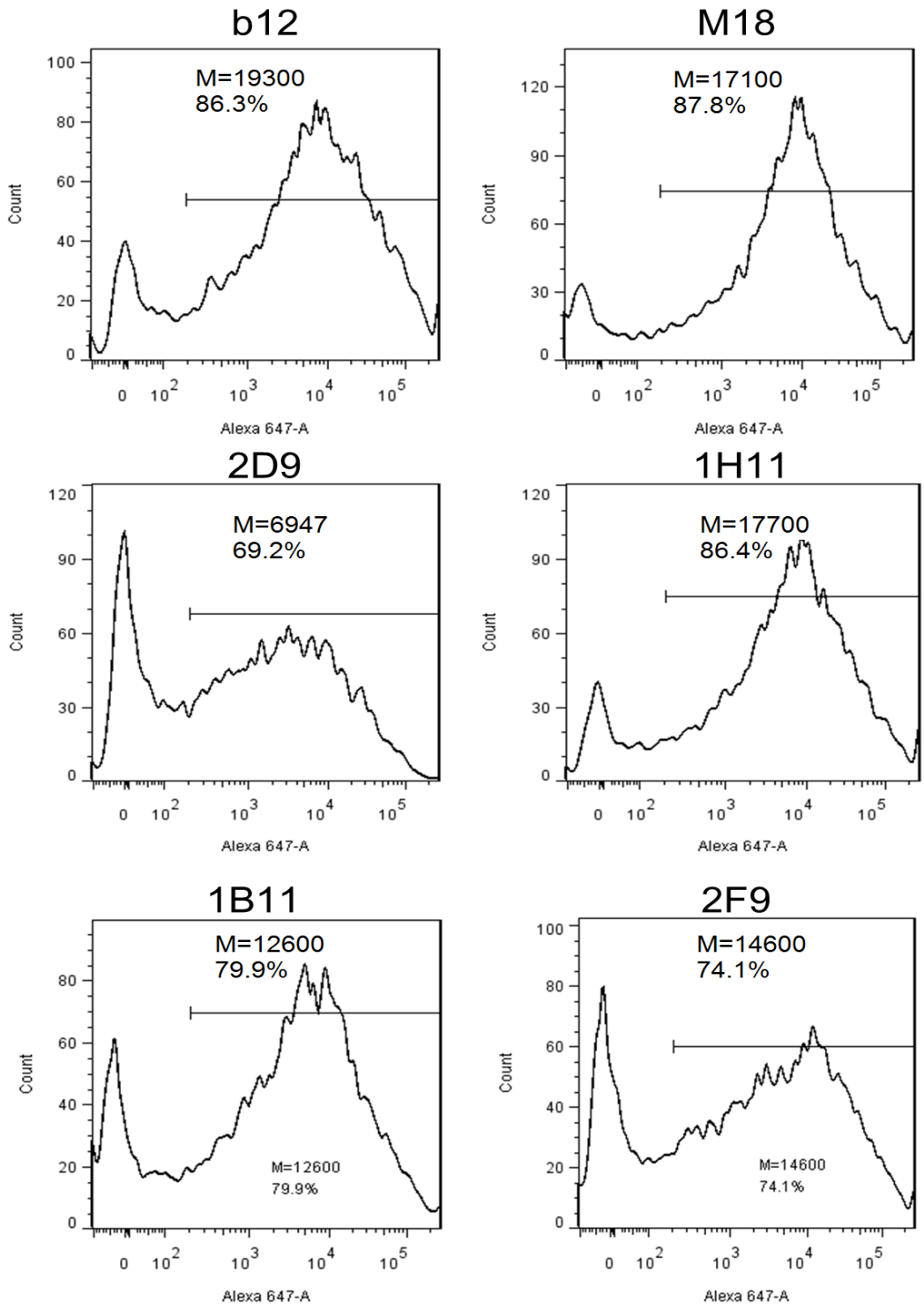

Figure 3.10 FACS scanning for antibody yeast surface display by labeling with chicken anti-c-Myc IgY then Alexa Fluor 647-goat anti-chicken IgG.

3.5 Identification of the binding clones

Fluorescence microscopy images of Alexa 488-MMP-14 labeled DX-2400, M18 and CD20 cells further confirmed DX-2400 scFv displayed on yeast surface can bind to MMP-14 (**Figure 3.11**). In the FITC channel, DX-2400 cells showed green rings, which were associated with cell rims as demonstrated in bright field channel. In contrast, cells displaying M18 or CD20 did not emit detectable fluorescence.

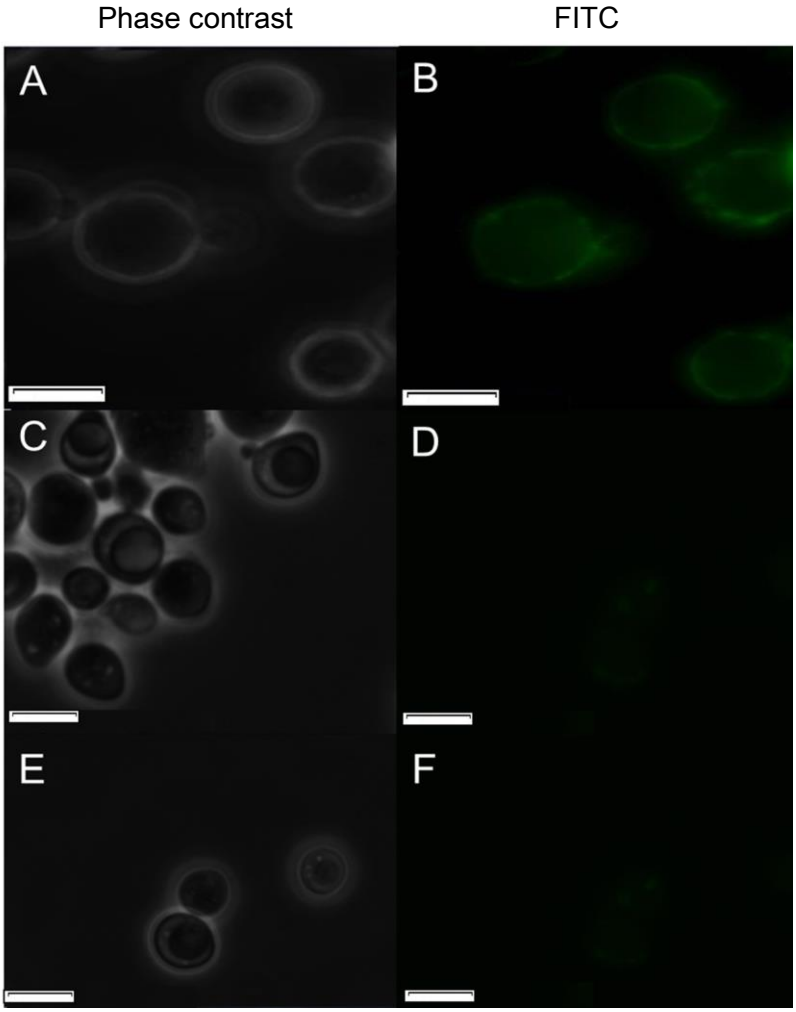

Figure 3.11 Microscopy images of yeast cells displaying different proteins. DX-2400 scFv **(A/B)**, M18 scFv **(C/D)**, CD20 **(E/F)**. Left, phase contrast microscopic images; Right, fluorescence microscopic images. Cells were labeled with Alexa-488-MMP-14. Bars are 5 μm.

Yeast cells displaying different antibodies were double-labeled with Alexa 488-MMP-14 for binding analysis, and chicken anti-c-Myc IgY/anti-chicken Alexa 647 IgG for expression analysis. Bivariate flow-cytometric scanning results suggested that MMP-14 specific clones can be clearly discriminated from non-binding clones (**Figure 3.12**). Yeast cells carrying DX-2400, 3B1, 2A10 or 1F8 scFv displaying plasmids had 54-59% of their populations located in the Q2 region, indicating that these scFvs were expressed and displayed on yeast surface at decent levels and bound to MMP-14, results consistent with our previous ELISA data (Nam et al., manuscript in preparation). While yeast cells displaying CD20, M18 scFv or b12 scFv had 47-53% of their populations located in the Q3 region, indicating that these non-relevant antibodies or CD20 were highly expressed and displayed on cell surface, but did not bind to MMP-14. And for the control clone (not transformed with any display plasmid), 80% of its population was located in the Q4 region, indicating low signals in both expression and MMP-14 binding.

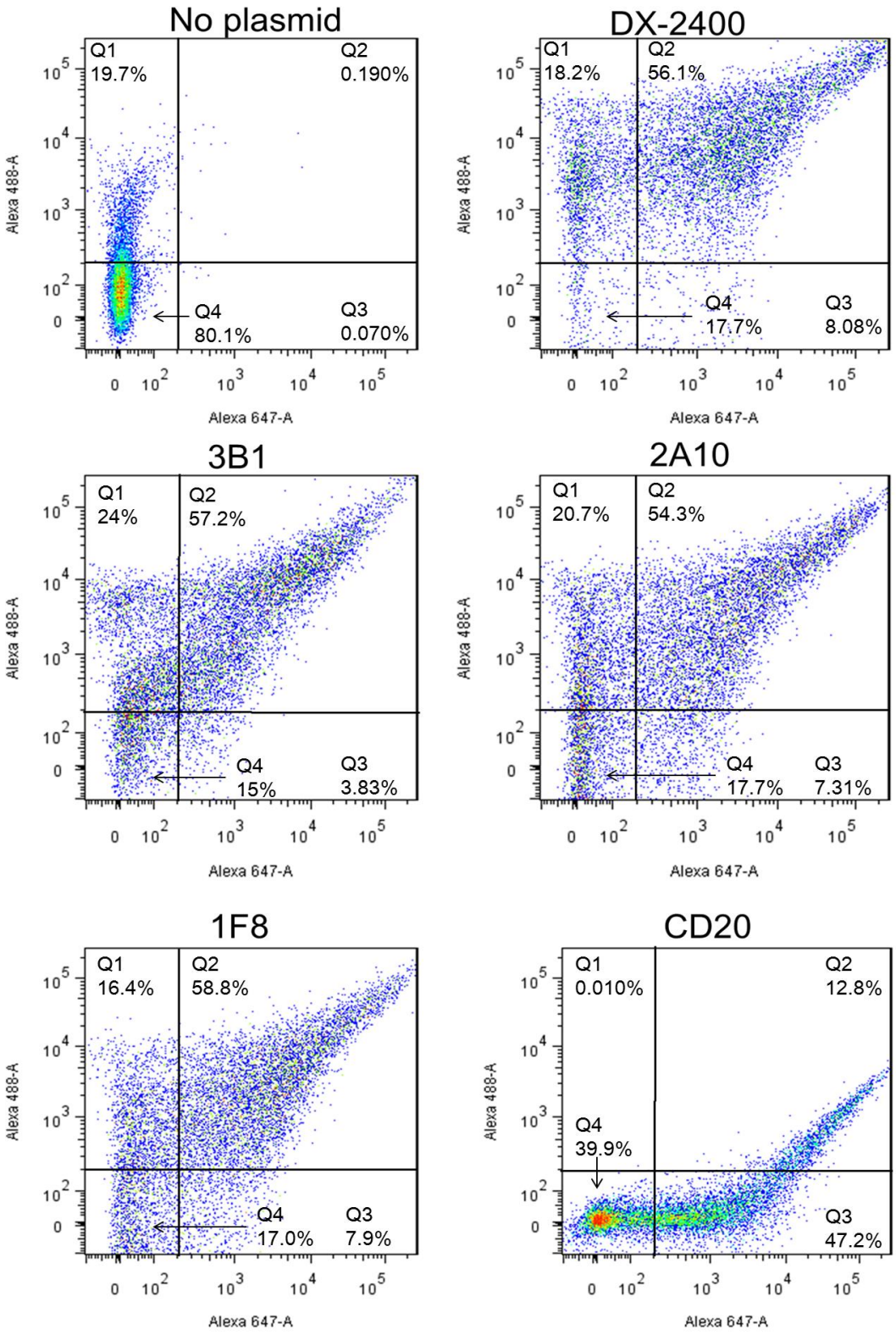
No plasmid
Q1
19.7%
Q2
0.190%
Q4
80.1%
Q3
0.070%
DX-2400
Q1
18.2%
Q2
56.1%
Q4
17.7%
Q3
8.08%
3B1
Q1
24%
Q2
57.2%
Q4
15%
Q3
3.83%
2A10
Q1
20.7%
Q2
54.3%
Q4
17.7%
Q3
7.31%
1F8
Q1
16.4%
Q2
58.8%
Q4
17.0%
Q3
7.9%
CD20
Q1
0.010%
Q2
12.8%
Q4
39.9%
Q3
47.2%
Alexa 488-A
Alexa 647-A
0
10^2
10^3
10^4
10^5

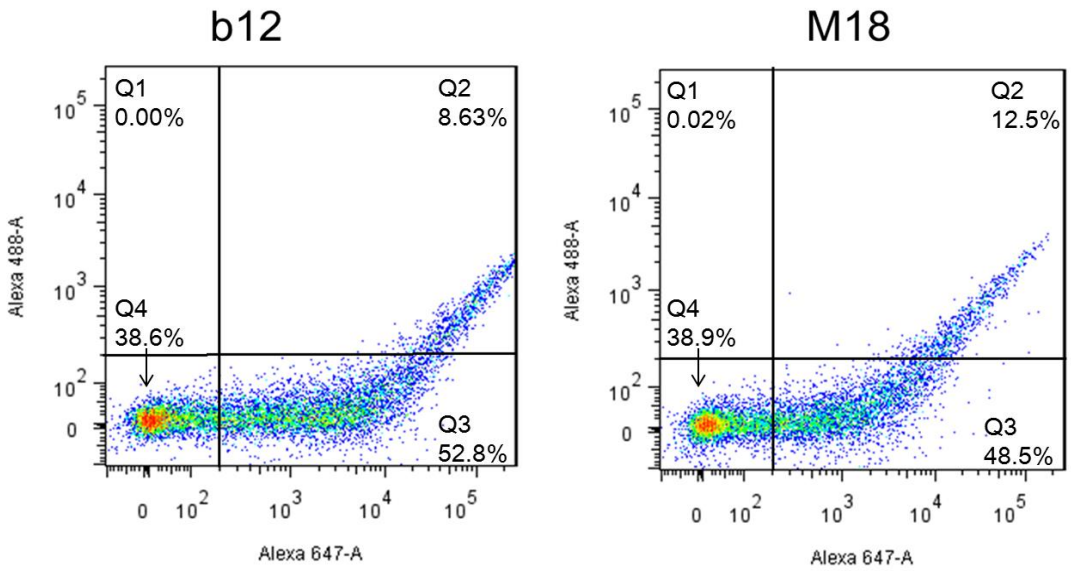

Figure 3.12 Identification of binding clones by dual color FACS.

3.6 Identification of the inhibitory clones by dual color FACS

Yeast cells carrying different scFv displaying plasmids were double-labeled with Alexa 488-MMP-14 and Alexa 647-N-TIMP-2, and subjected for dual color flow cytometric scanning analysis. Three scenarios are expected (**Figure 3.13**): **(Scenario 1)** inhibitory clones, which bind to MMP-14 at the epitopes overlapping with the region where TIMP-2 inhibits at, therefore associated with high Alexa 488 signals and low Alexa 647 signals; **(Scenario 2)** MMP-14 specific but non-inhibitory clones, which bind to MMP-14 at the epitopes other than the region where TIMP-2 inhibits at, therefore associated with high signals on both fluorescence channels; **(Scenario 3)** non-binding clones, which cannot bind to MMP-14, therefore associated with low signals in both fluorescence channels.

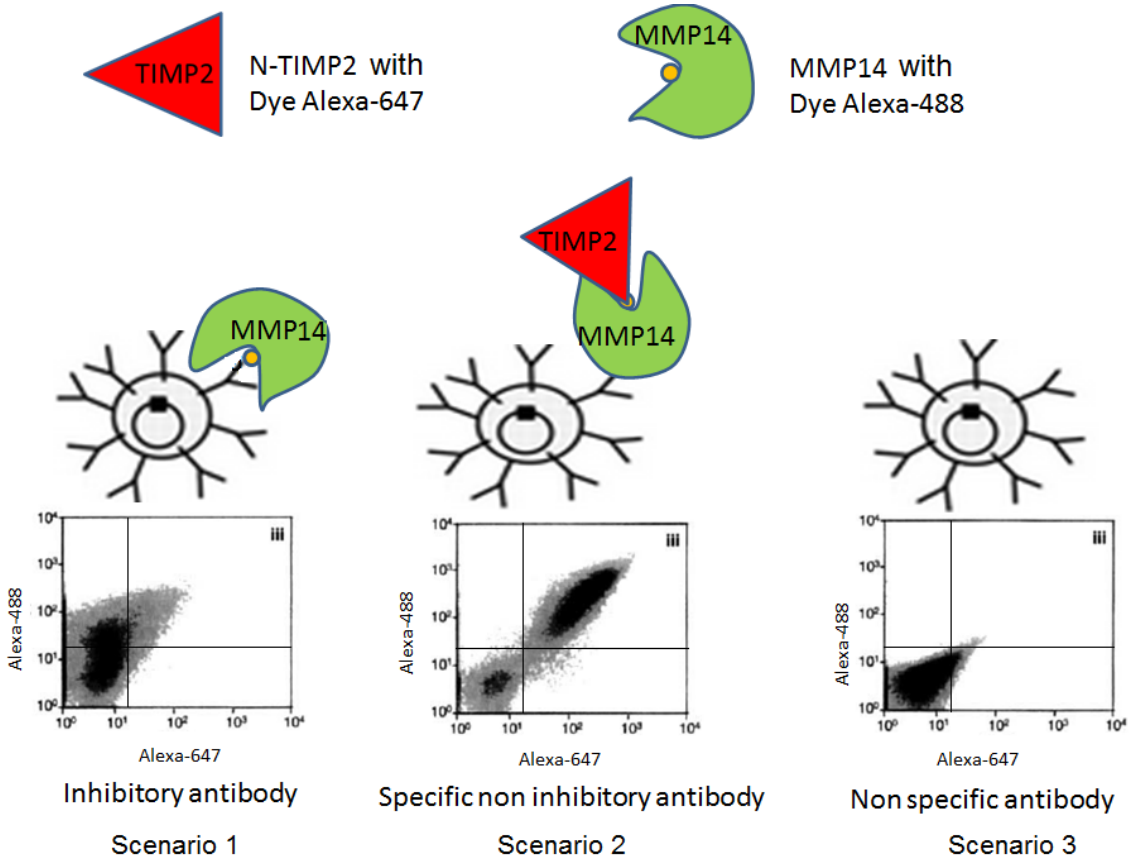

Figure 3.13 Distinguish inhibitory clones from non-specific or non-inhibitory clones by dual color labeling and FACS scanning.

Experimental results demonstrated that incubation with fluorescent dye conjugated MMP-14 and TIMP-2 followed by dual color FACS scanning can clearly distinguish inhibitory clones from non-specific or non-inhibitory clones (**Figure 3.14**). As negative controls, yeast cells without plasmids or carrying the CD20 display plasmid had 88-91% of their populations in the region of Q4, indicating low fluorescence signals on both Alexa 488 and Alexa 647 channels, thus they are non-specific clones (**Scenario 3**). Yeast cells carrying display plasmids for scFvs of M18, b12, 2F9, 2D9, 1H11 or 1B11 had 93-96% of their populations located in the region Q4, therefore they are non-specific antibodies to MMP-14 (**Scenario 3**), results consistent with our previous ELISA

data (Nam et al., manuscript in preparation). Antibody clone 2A10 was isolated as a high affinity binder from a synthetic antibody library by phage panning against MMP-14 (Nam et al., manuscript in preparation). Dual color FACS scanning of 2A10 clone showed 73% of its population was located in Q2, indicating high signals in both Alexa 488 and Alexa 647 channels, confirmed that 2A10 was a specific but non-inhibitory clone (**Scenario 2**). As a positive control, yeast cells carrying the MMP-14 inhibitory antibody DX-2400 showed 78% of its population was located in the region Q1, indicating a high signal in Alexa 488 and a low signal in Alexa 647 and confirming it is an inhibitory clone (**Scenario 1**). Our previous phage panning experiments have isolated a putative inhibitory clone 1F8, which exhibited a strong ELISA signal and inhibited MMP-14 in enzymatic assays. The dual color scanning results of 1F8 showed 30% of its population was located in region Q1 (**Scenario 1**) with only 5% of its population located in region Q2 indicting 1F8 was significantly different from the specific but non-inhibitory clones like 2A10 (**Scenario 2**). Notable, 65% of 1F8 population was located in region Q4 (**Scenario 3**), presumably due to lower expression level than that of DX-2400. Similarly, antibody clone 3B1 isolated from phage panning also had considerable amount of cells located in region Q1 (15%) with majority of its population located in Q4 (79%).

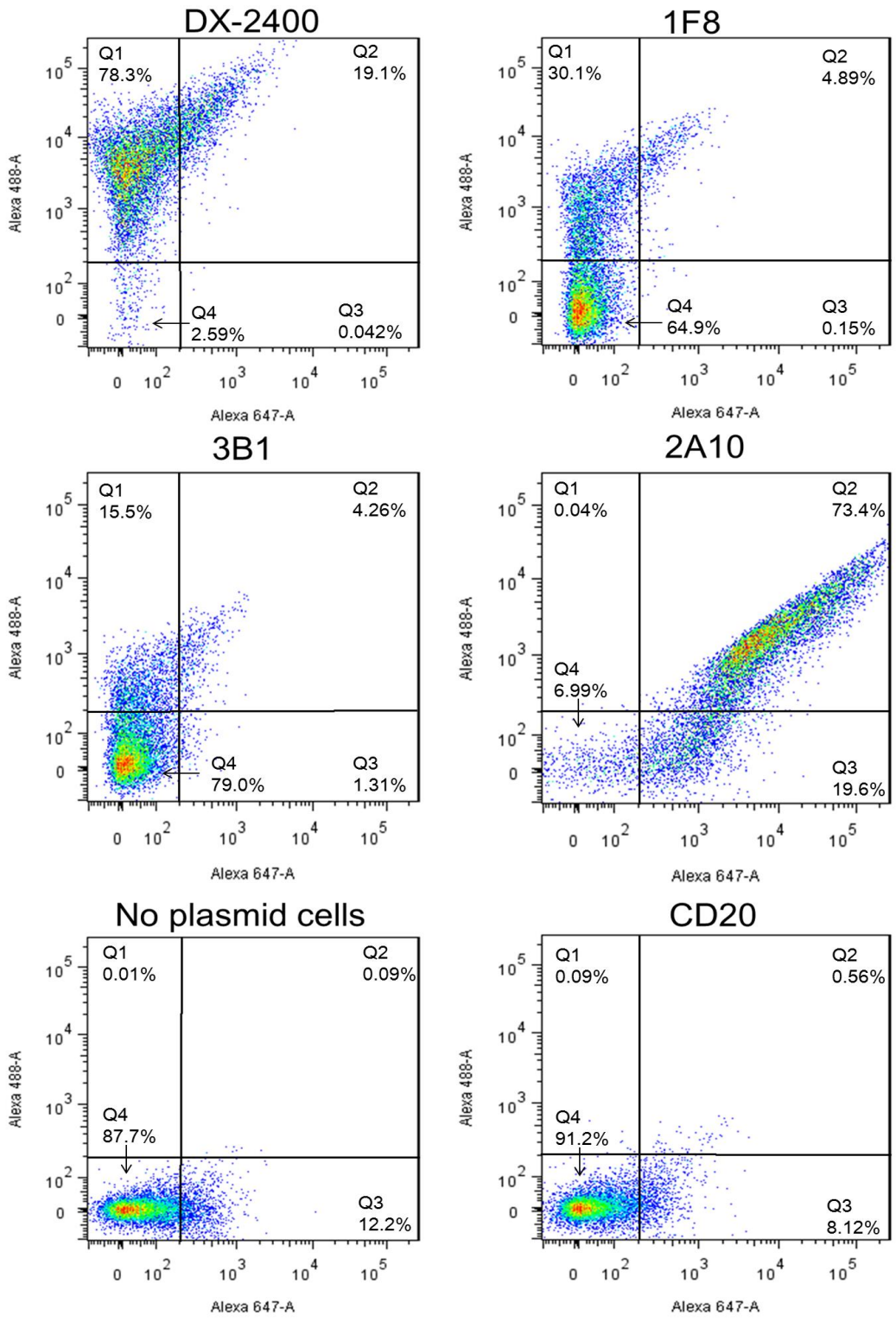
DX-2400
Q1
78.3%
Q2
19.1%
Q4
2.59%
Q3
0.042%
1F8
Q1
30.1%
Q2
4.89%
Q4
64.9%
Q3
0.15%
3B1
Q1
15.5%
Q2
4.26%
Q4
79.0%
Q3
1.31%
2A10
Q1
0.04%
Q2
73.4%
Q4
6.99%
Q3
19.6%
No plasmid cells
Q1
0.01%
Q2
0.09%
Q4
87.7%
Q3
12.2%
CD20
Q1
0.09%
Q2
0.56%
Q4
91.2%
Q3
8.12%
Alexa 488-A
Alexa 647-A

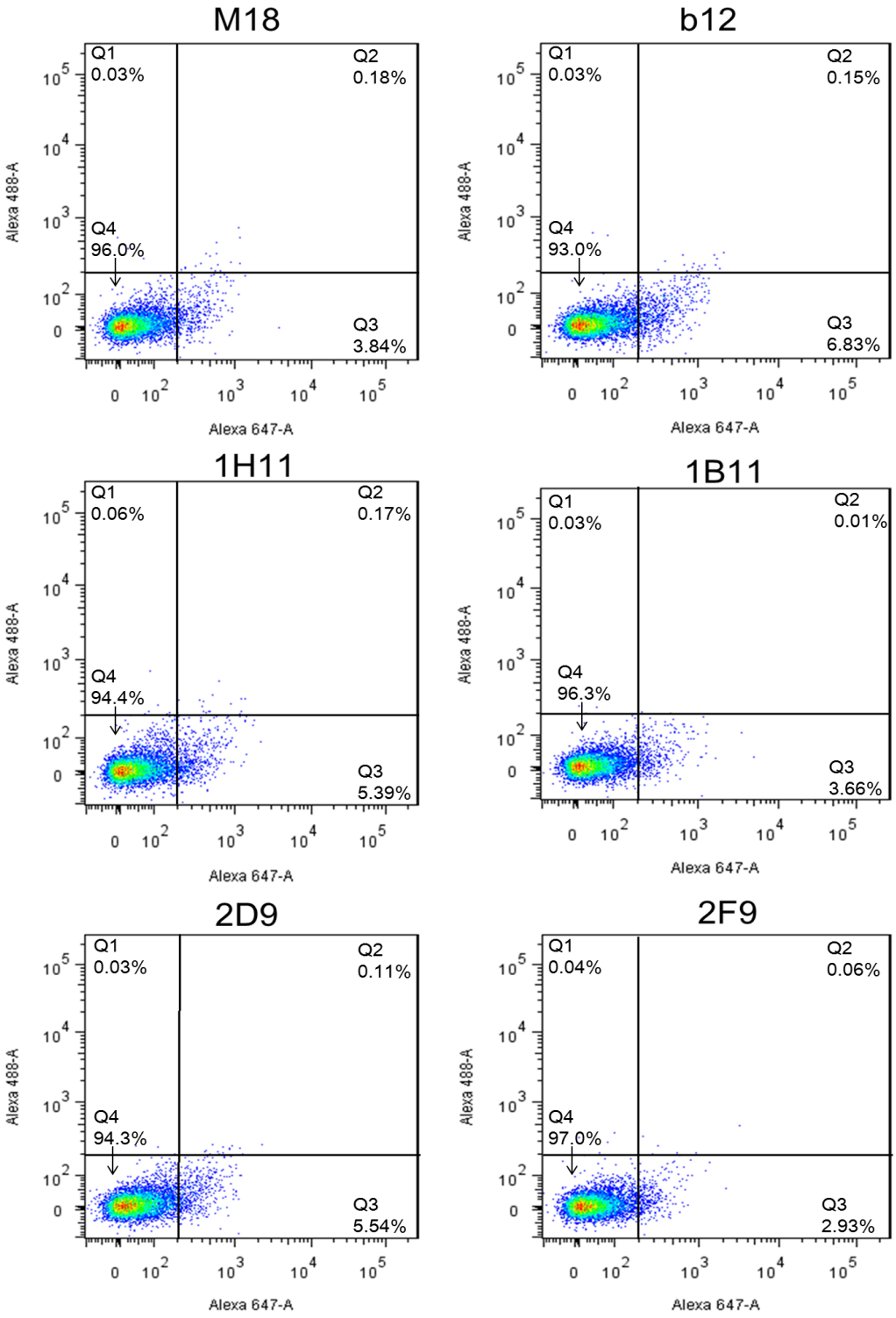

Figure 3.14 Identification of the inhibitory clones by dual color FACS (1st attempt).

To further prove the likelihoods of 1F8 and 3B1 as MMP-14 inhibitory clones, dual color labeling and FACS scanning were repeated for these suspicious clones as well as controls. The voltages of Alexa 488 and Alexa 647 were increased to be 560 and 775, from 350 and 632 in the first attempt (**Figure 3.15**). The new FACS scanning results (**Figure 3.15**) confirmed again that M18, b12, 2F9, 2D9, 1H11 and 1B11 were non-specific clones and 1F8 and DX-2400 were inhibitory clones, the same results as previous tests (**Figure 3.14**). And 3B1 had 78% of its population located in region Q2, a result very similar to that of 2A10 (73% in Q2), suggesting that 3B1 was a MMP-14 specific but non-inhibitory clone. To validate 1F8 and 3B1, further FACS tests using various concentrations of MMP-14 and TIMP-2 and/or other biochemical analyses are required and these experiments will be subject for future studies.

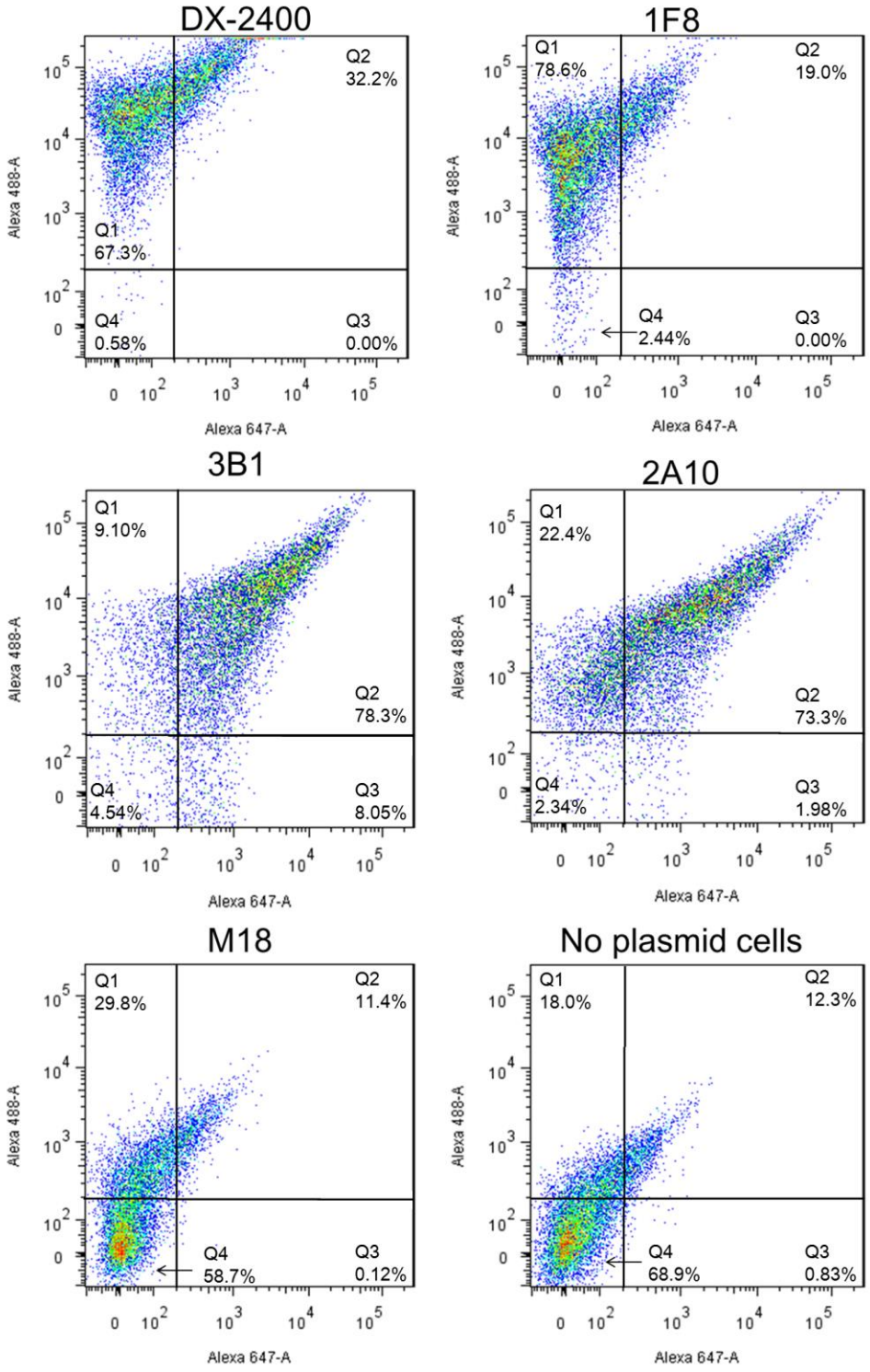

Figure 3.15 Identification of the inhibitory clones by dual color FACS (2nd Attempt).

4 Conclusions

The main contribution of this thesis is the validation that inhibitory antibodies can be distinguished from non-specific or non-inhibitory clones by FACS (fluorescence-activated cell sorting), therefore paving the road for future study on selection of inhibitory antibodies from combinatorial libraries. This was achieved by labeling the target MMP-14 (matrix metalloproteinase 14) with fluorophore Alexa 488 and its native inhibitor TIMP-2 (Tissue inhibitor of metalloproteinase 2) with fluorophore Alexa 647, and then followed by dual color FACS scanning of yeast cells on which the control scFv antibodies were surface displayed. Inhibitory antibodies DX-2400 and 1F8 exhibited high signal on Alexa488-MMP-14 and low signal on Alexa647-TIMP-2, while non-specific clones M18, etc. exhibited low signals both fluorophores, and specific but non-inhibitory clones exhibited high signals on both fluorophores. The detailed results were shown as the following:

1) The catalytic domain of MMP-14 was expressed, purified and refolded to its active format, demonstrated by SDS-PAGE and enzymatic FRET assays using fluorescence substrates.
2) Expression plasmid for N-terminal domain of TIMP-2 was constructed based on pET32b. N-TIMP-2 was expressed, purified and refolded to its active format with desired inhibition functions on MMP-14 showed by FRET assay.
3) Produced MMP-14 and N-TIMP-2 were conjugated with fluorescence Alexa 488 and Alexa 647 respectively with desired degrees of labeling validated by SDS-PAGE gel and UV absorbance. Dye conjugated MMP-14 maintains its activity similar to that of

non-conjugated MMP-14, and conjugated N-TIMP-2 remains its inhibition function with lower but acceptable activity.

4) Several antibodies clones (DX-2400, 1F8, M18, b12, 2A10, 3B1, 1B11, 1H11, 2D9, 2F9) were converted to their scFv formats, cloned into yeast display vector pCTCON-2. These antibodies were displayed at yeast surface with decent expression levels, proved by FACS scan after labeling with chicken anti-c-Myc IgY anti-chicken Alexa 647 IgG.
5) MMP-14 specific clones were identified by labeling with Alexa488-MMP-14 and chicken anti-c-Myc IgY/anti-chicken Alexa 647 IgG (for expression), followed by dual color FACS scan. MMP-14 specific antibodies (DX-2400, 1F8, 2A10, 3B1) showed high signals on both Alexa488 and Alexa647 fluorophores, while nonspecific antibody (M18, b12) only showed antibody expression and display but had low signal on Alexa488-MMP-14.
6) By labelling with Alexa488-MMP-14 and Alexa647-N-TIMP-2, inhibitory antibodies (DX-2400, 1F8) exhibited high signal on Alexa488-MMP-14 and low signal on Alexa647-N-TIMP-2, while non-specific antibody cells (M18, b12, 3B1, 1B11, 1H11, 2D9, 2F9) exhibited high signals on both fluorophores and specific but non-inhibitory antibodies (3B1, 2A10) exhibited low signals on both fluorophores.

5 Future Works

This study has validated that yeast cells displaying inhibitory antibodies can be clearly distinguished from non-specific or non-inhibitory clones. For further utilizing this function-based rather than binding-based screening method to select *de novo* inhibitory antibodies from combinatorial libraries, the following investigations need to undertake:

(1) Isolate inhibitory clones from artificially spiked mixtures made of DX-2400 (or 1F8), 3B1, 2A10 and M18 at molar ratios of 1:10:10:10, 1:100:100:100, $1:10^3:10^3:10^3$) by labeling and dual color sorting.

(2) The conditions of labeling and FACS sorting procedures will need to be optimized to minimize the population overlapping between inhibitory clones and non-inhibitory/nonspecific clones.

(3) Affinity maturation of previously isolated inhibitory clones (DX-2400 and 1F8) to improve their inhibition activities.

6 Reference

Becker, S., Schmoldt, H. U., Adams, T. M., Wilhelm, S., & Kolmar, H. (2004). Ultra-high-throughput screening based on cell-surface display and fluorescence-activated cell sorting for the identification of novel biocatalysts. *Current opinion in biotechnology*, *15*(4), 323-329.

Bird, R. E., Hardman, K. D., Jacobson, J. W., Johnson, S., Kaufman, B. M., Lee, S. M., Lee, T., Pope, H. S., Riordan, G. S., & Whitlow, M. (1988). Single-chain antigen-binding proteins. *Science*, *242*(4877), 423-426.

Boder, E. T., & Wittrup, K. D. (1997). Yeast surface display for screening combinatorial polypeptide libraries. *Nature biotechnology*, *15*(6), 553-557.

Bonner, W. A., Hulett, H. R., Sweet, R. G., & Herzenberg, L. A. (1972). Fluorescence activated cell sorting. *Review of Scientific Instruments*, *43*(3), 404-409.

Cacia, J., Keck, R., Presta, L. G., & Frenz, J. (1996). Isomerization of an aspartic acid residue in the complementarity-determining regions of a recombinant antibody to human IgE: identification and effect on binding affinity. *Biochemistry*, *35*(6), 1897-1903.

Chambers, A. F., & Matrisian, L. M. (1997). Changing views of the role of matrix metalloproteinases in metastasis. *Journal of the National Cancer Institute*, *89*(17), 1260-1270.

Chao, G., Lau, W. L., Hackel, B. J., Sazinsky, S. L., Lippow, S. M., & Wittrup, K. D. (2006). Isolating and engineering human antibodies using yeast surface display. *Nature protocols*, *1*(2), 755-768.

Cormack, B. P., Valdivia, R. H., & Falkow, S. (1996). FACS-optimized mutants of the green fluorescent protein (GFP). *Gene*, *173*(1), 33-38.

Decock, J., Thirkettle, S., Wagstaff, L., & Edwards, D. R. (2011). Matrix metalloproteinases: protective roles in cancer. *Journal of cellular and molecular medicine*, *15*(6), 1254-1265.

Devy, L., Huang, L., Naa, L., Yanamandra, N., Pieters, H., Frans, N., ... & Dransfield, D. T. (2009). Selective inhibition of matrix metalloproteinase-14 blocks tumor growth, invasion, and angiogenesis. *Cancer research*, *69*(4), 1517-1526.

Egeblad, M., & Werb, Z. (2002). New functions for the matrix metalloproteinases in cancer progression. *Nature Reviews Cancer*, *2*(3), 161-174.

Feldhaus, M. J., Siegel, R. W., Opresko, L. K., Coleman, J. R., Feldhaus, J. M. W., Yeung, Y. A., Cochran, J. R., Heinzelman, P., Colby, D., Swers, J., Graff, C., Wiley, H . S., & Wittrup, K. D. (2003). Flow-cytometric isolation of human antibodies from a

nonimmune Saccharomyces cerevisiae surface display library. *Nature biotechnology*, *21*(2), 163-170.

Fernandez-Catalan, C., Bode, W., Huber, R., Turk, D., Calvete, J. J., Lichte, A., Tschesche, H., & Maskos, K. (1998). Crystal structure of the complex formed by the membrane type 1-matrix metalloproteinase with the tissue inhibitor of metalloproteinases-2, the soluble progelatinase A receptor. *The EMBO journal*, *17*(17), 5238-5248.

Francisco, J. A., Campbell, R., Iverson, B. L., & Georgiou, G. (1993). Production and fluorescence-activated cell sorting of Escherichia coli expressing a functional antibody fragment on the external surface. *Proceedings of the National Academy of Sciences*, *90*(22), 10444-10448.

Fu, A. Y., Spence, C., Scherer, A., Arnold, F. H., & Quake, S. R. (1999). A microfabricated fluorescence-activated cell sorter. *Nature biotechnology*, *17*(11), 1109-1111.

Harris, R. J., Shire, S. J., & Winter, C. (2004). Commercial manufacturing scale formulation and analytical characterization of therapeutic recombinant antibodies. *Drug development research*, *61*(3), 137-154.

Herzenberg, L. A., Parks, D., Sahaf, B., Perez, O., Roederer, M., & Herzenberg, L. A. (2002). The history and future of the fluorescence activated cell sorter and flow cytometry: a view from Stanford. *Clinical chemistry*, *48*(10), 1819-1827.

Hidalgo, M., & Eckhardt, S. G. (2001). Development of matrix metalloproteinase inhibitors in cancer therapy. *Journal of the National Cancer Institute*, *93*(3), 178-193.

Hoogenboom, H. R. (2005). Selecting and screening recombinant antibody libraries. *Nature biotechnology*, *23*(9), 1105-1116.

Hoogenboom, H. R., Griffiths, A. D., Johnson, K. S., Chiswell, D. J., Hudson, P., & Winter, G. (1991). Multi-subunit proteins on the surface of filamentous phage: methodologies for displaying antibody (Fab) heavy and light chains. *Nucleic Acids Research*, *19*(15), 4133-4137.

Janeway, C. A., Travers, P., Walport, M. J., & Shlomchik, M. J. (2001). *Immunobiology: the immune system in health and disease* (Vol. 2). Churchill Livingstone.

Julius, M. H., Masuda, T., & Herzenberg, L. A. (1972). Demonstration that antigen-binding cells are precursors of antibody-producing cells after purification with a fluorescence-activated cell sorter. *Proceedings of the National Academy of Sciences*, *69*(7), 1934-1938.

Kessenbrock, K., Plaks, V., & Werb, Z. (2010). Matrix metalloproteinases: regulators of the tumor microenvironment. *Cell*, *141*(1), 52-67.

Kondo, A., & Ueda, M. (2004). Yeast cell-surface display-applications of molecular display. *Applied microbiology and biotechnology*, *64*(1), 28-40.

Koo, H. M., Kim, J. H., Hwang, I. K., Lee, S. J., Kim, T. H., Rhee, K. H., & Lee, S. T. (2002). Refolding of the catalytic and hinge domains of human MT1-mMP expressed in Escherichia coli and its characterization. *Molecules and cells*,*13*(1), 118-124.

Lichte, A., Kolkenbrock, H., & Tschesche, H. (1996). The recombinant catalytic domain of membrane-type matrix metalloproteinase-1 (MT1-MMP) induces activation of progelatinase A and progelatinase A complexed with TIMP-2. *FEBS letters*, *397*(2), 277-282.

Mitra, D. K., De Rosa, S. C., Luke, A., Balamurugan, A., Khaitan, B. K., Tung, J., ... & Roederer, M. (1999). Differential representations of memory T cell subsets are characteristic of polarized immunity in leprosy and atopic diseases.*International immunology*, *11*(11), 1801-1810.

Murphy, G., & Knäuper, V. (1997). Relating matrix metalloproteinase structure to function: why the "hemopexin" domain?. *Matrix biology*, *15*(8), 511-518.

Murphy, G., Stanton, H., Cowell, S., Butler, G., Knauper, V., Atkinson, S., Gavrilovic, J. (1999). Mechanisms for pro matrix metalloproteinase activation. *Apmis*, *107*(1−6), 38-44.

Murphy, G., Willenbrock, F., Ward, R. V., Cockett, M. I., Eaton, D., & Docherty, A. J. (1992). The C-terminal domain of 72 kDa gelatinase A is not required for catalysis, but is essential for membrane activation and modulates interactions with tissue inhibitors of metalloproteinases. *Biochem. j*, *283*, 637-641.

Nakahara, H., Howard, L., Thompson, E. W., Sato, H., Seiki, M., Yeh, Y., & Chen, W. T. (1997). Transmembrane/cytoplasmic domain-mediated membrane type 1-matrix metalloprotease docking to invadopodia is required for cell invasion. *Proceedings of the National Academy of Sciences*, *94*(15), 7959-7964.

Nam, D. H., & Ge, X. (2013). Development of a periplasmic FRET screening method for protease inhibitory antibodies. *Biotechnology and bioengineering*, *110*(11), 2856-2864.

Ndinguri, M. W., Bhowmick, M., Tokmina-Roszyk, D., Robichaud, T. K., & Fields, G. B. (2012). Peptide-based selective inhibitors of matrix metalloproteinase-mediated activities. *Molecules*, *17*(12), 14230-14248.

Overall, C. M., & Kleifeld, O. (2006). Towards third generation matrix metalloproteinase inhibitors for cancer therapy. *British journal of cancer*, *94*(7), 941-946.

Parks, D. R., Bryan, V. M., Oi, V. T., & Herzenberg, L. A. (1979). Antigen-specific identification and cloning of hybridomas with a fluorescence-activated cell sorter. *Proceedings of the National Academy of Sciences*, *76*(4), 1962-1966.

Peterson, E., Owens, S. M., & Henry, R. L. (2008). Monoclonal antibody form and function: manufacturing the right antibodies for treating drug abuse. In *Drug Addiction* (pp. 87-100). Springer New York.

Reichert, J. M. (2008). Monoclonal antibodies as innovative therapeutics. *Current pharmaceutical biotechnology*, *9*(6), 423-430.

Sato, H., Takino, T., Okada, Y., Cao, J., Shinagawa, A., Yamamoto, E., & Seiki, M. (1994). A matrix metalloproteinase expressed on the surface of invasive tumour cells. *Nature*, *370*(6484), 61-65.

Shiryaev, S. A., Remacle, A. G., Golubkov, V. S., Ingvarsen, S., Porse, A., Behrendt, N., Cieplak, P., & Strongin, A. Y. (2013). A monoclonal antibody interferes with TIMP-2 binding and incapacitates the MMP-2-activating function of multifunctional, pro-tumorigenic MMP-14/MT1–MMP. *Oncogenesis*, *2*(12), e80.

Smith, G. P., & Petrenko, V. A. (1997). Phage display. *Chemical reviews*,*97*(2), 391-410.
Smith, G. P. (1985). Filamentous fusion phage: novel expression vectors that display cloned antigens on the virion surface. *Science*, *228*(4705), 1315-1317.

Sternlicht, M. D., & Werb, Z. (2001). How matrix metalloproteinases regulate cell behavior. *Annual review of cell and developmental biology*, *17*, 463.

Takemoto, N., Tada, M., Hida, Y., Asano, T., Cheng, S., Kuramae, T., Hamadaa, J., Miyamoto, M., Kondo, S., & Moriuchi, T. (2007). Low expression of reversion-inducing cysteine-rich protein with Kazal motifs (RECK) indicates a shorter survival after resection in patients with adenocarcinoma of the lung. *Lung Cancer*, *58*(3), 376-383.

Tomari, T., Koshikawa, N., Uematsu, T., Shinkawa, T., Hoshino, D., Egawa, N., Isobe, T., & Seiki, M. (2009). High throughput analysis of proteins associating with a proinvasive MT1‐MMP in human malignant melanoma A375 cells. *Cancer science*, *100*(7), 1284-1290.

Turk, B. (2006). Targeting proteases: successes, failures and future prospects. *Nature reviews Drug discovery*, *5*(9), 785-799.

Wang, W., Singh, S., Zeng, D. L., King, K., & Nema, S. (2007). Antibody structure, instability, and formulation. *Journal of pharmaceutical sciences*, *96*(1), 1-26.

Willenbrock, F., Crabbe, T., Slocombe, P. M., Sutton, C. W., Docherty, A. J., Cockett, M. I., O'Shea, M., Brocklehurst, K., Phillips, I. R., & Murphy, G. (1993). The activity of the tissue inhibitors of metalloproteinases is regulated by C-terminal domain interactions: a kinetic analysis of the inhibition of gelatinase A. *Biochemistry*, *32*(16), 4330-4337.

Wu, T. T., & Kabat, E. A. (1970). An analysis of the sequences of the variable regions of Bence Jones proteins and myeloma light chains and their implications for antibody complementarity. *The Journal of experimental medicine*, *132*(2), 211-250.

Zucker, S., & Cao, J. (2009). Selective matrix metalloproteinase (MMP) inhibitors in cancer therapy. *Cancer biology & therapy*, *8*(24), 2371-2373.

Zucker, S., Hymowitz, M., Conner, C., Zarrabi, H. M., Hurewitz, A. N., Matrisian, L., Boyd, D., Nicholson, G., & Montana, S. (1999). Measurement of matrix metalloproteinases and tissue inhibitors of metalloproteinases in blood and tissues: clinical and experimental applications. *Annals of the New York Academy of Sciences*, *878*(1), 212-227.

Zucker, S., Pei, D., Cao, J., & Lopez-Otin, C. (2003). Membrane type-matrix metalloproteinases (MT-MMP). *Current topics in developmental biology*, *54*, 1-74.

7 Appendices

Appendix 1 N-TIMP-2 sequencing result compared with reported TIMP-2 by using CLUSTAL 2.1 (www.ebi.ac.uk/Tools/msa/clustalw2/)

```
N-TIMP-2        TGTAGCTGCAGTCCGGTGCATCCGCAGCAGGCGTTTTGCAATGCCGATATTGTGATTCGT
60
sequencing      TGTAGCTGCAGTCCGGTGCATCCGCAGCAGGCGTTTTGCAATGCCGATATTGTGATTCGT
60
                ************************************************************

N-TIMP-2        GCGAAAGCGGTGAACAAAAAGGAAGTGGATAGCGGCAACGATATCTATGGCAATCCGATT
120
sequencing      GCGAAAGCGGTGAACAAAAAGGAAGTGGATAGCGGCAACGATATCTATGGCAATCCGATT
120
                ************************************************************

N-TIMP-2        AAACGTATTCAGTATGAAATAAAGCAGATCAAAATGTTTAAAGGCCCGGATCAGGACATT
180
sequencing      AAACGTATTCAGTATGAAATAAAGCAGATCAAAATGTTTAAAGGCCCGGATCAGGACATT
180
                ************************************************************

N-TIMP-2        GAGTTCATTTATACCGCACCGGCAGCAGCGGTGTGCGGCGTGAGCCTGGATATTGGCGGC
240
sequencing      GAGTTCATTTATACCGCACCGGCAGCAGCGGTGTGCGGCGTGAGCCTGGATATTGGCGGC
240
                ************************************************************

N-TIMP-2        AAAAAAGAATATCTGATTGCGGGCAAAGCGGAAGGCAATGGCAACATGCACATAACCCTG
300
sequencing      AAAAAAGAATATCTGATTGCGGGCAAAGCGGAAGGCAATGGCAACATGCACATAACCCTG
300
                ************************************************************

N-TIMP-2        TGCGATTTCATTGTGCCGTGGGATACCCTGAGCGCGACCCAGAAAAAAAGCCTGAATCAT
360
sequencing      TGCGATTTCATTGTGCCGTGGGATACCCTGAGCGCGACCCAGAAAAAAAGCCTGAATCAT
360
                ************************************************************

N-TIMP-2        CGTTATCAGATGGGCTGC 378
sequencing      CGTTATCAGATGGGCTGC 378
                ******************
```

Appendix 2 N-TIMP-2 inhibition assays at different substrate concentrations

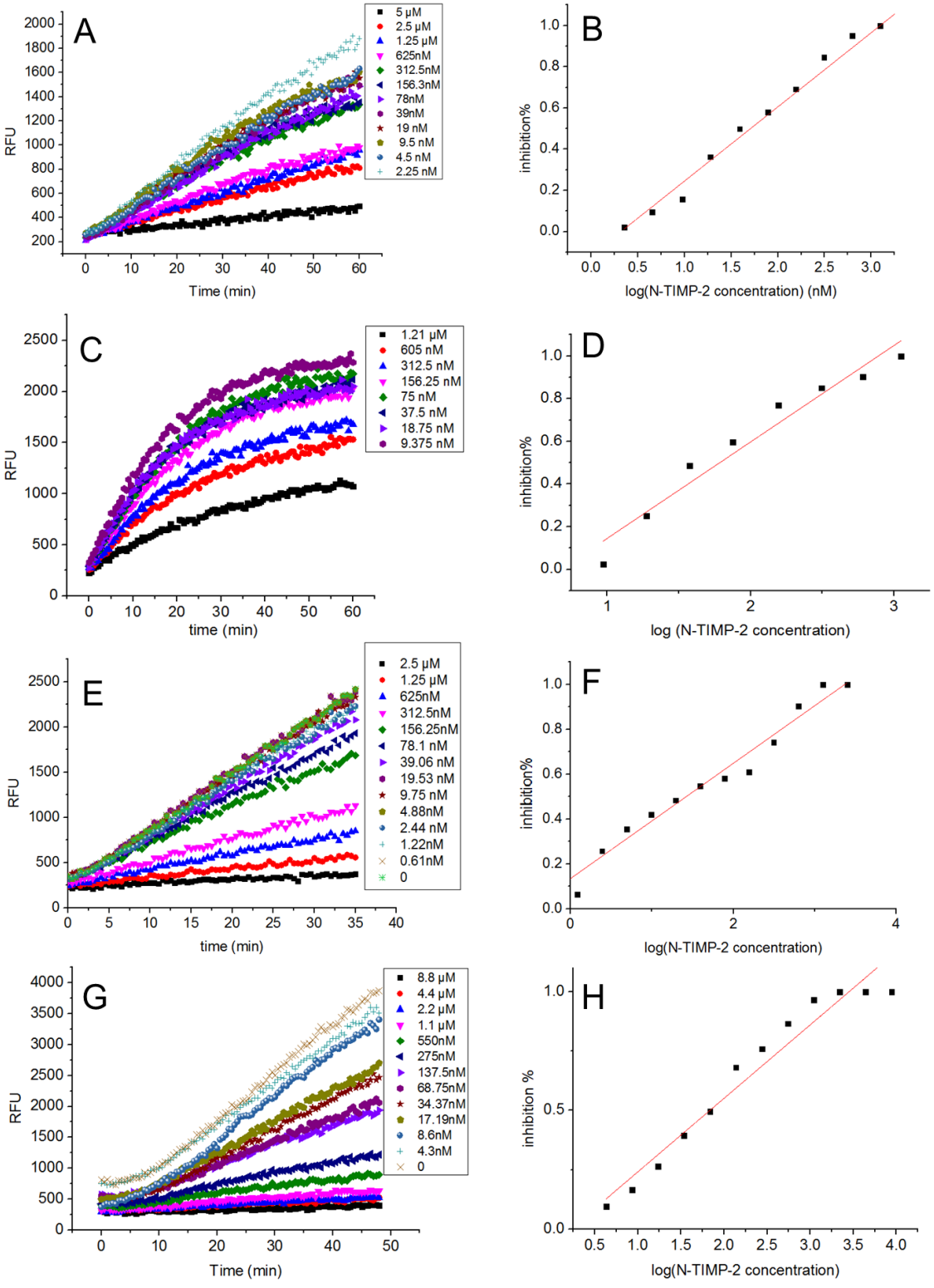

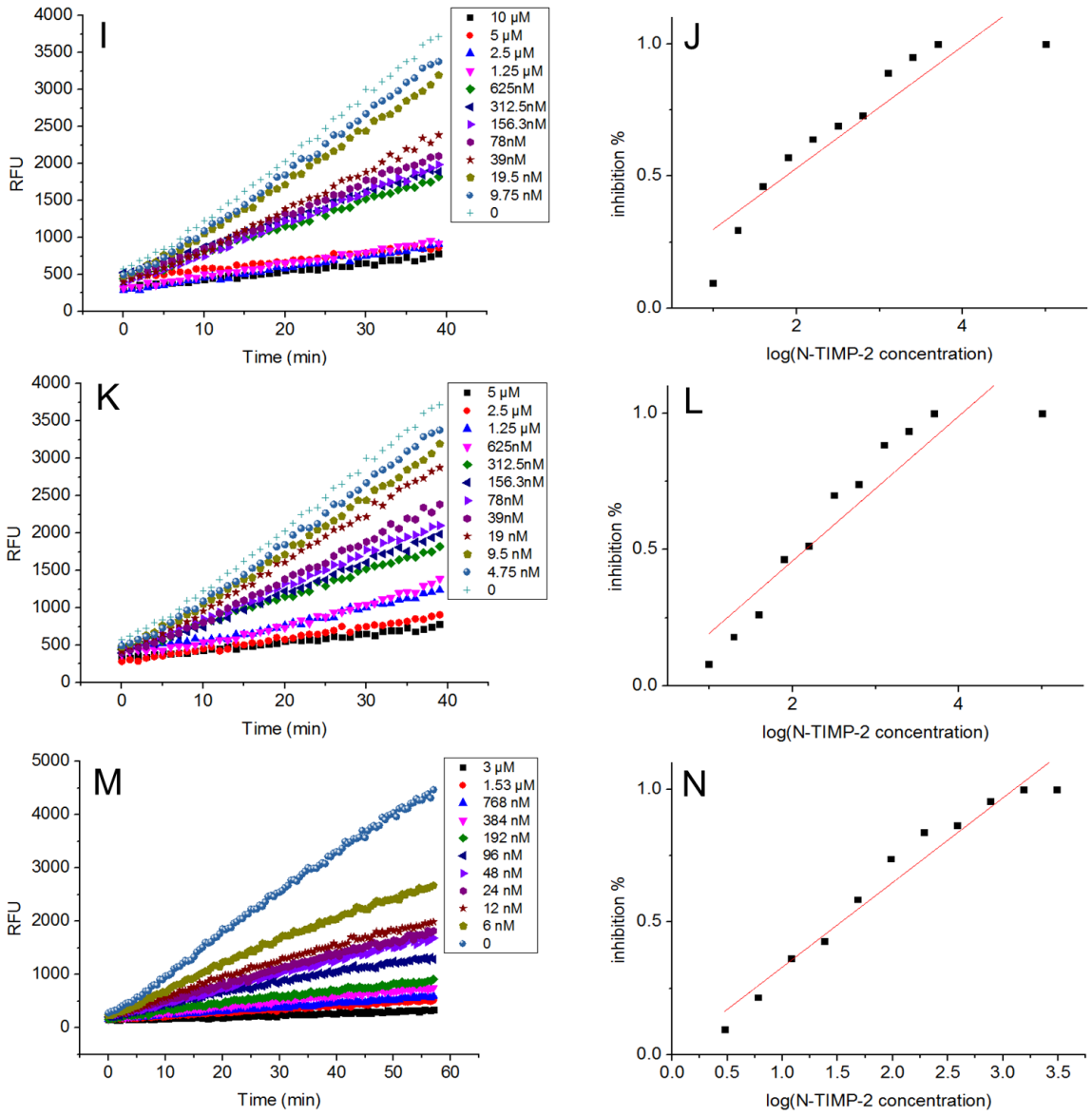

Figure 7.1 N-TIMP-2 inhibition curves and IC_{50} estimations for 2 nM MMP-14 with various substrate concentrations. 0.3 µM **(A/B)**, 0.6 µM **(C/D)**,1 µM **(E/F)**, 1.5 µM **(G/H)**, 2 µM **(I/J)**, 3.8 µM **(K/L)**, substrate. 4 µM **(M/N)**.